to maintain the all-trans planar geometry of the coordinated ring of L, the CF_3 group of the phosphorus atom at the apex must sit over the metal as it does in the structure of II. The crystal structure of the complex *cis*-$[IrBr(CO)\{C(CN)_2{=}C(CN)_2\}(PPh_3)_2]$[19] shows that the sites above and below the M(TCNE)$(PPh_3)_2$ plane are blocked by CO and Br ligands, so that the CF_3 group of the ligand L cannot be accommodated without distorting the framework. The lack of complex formation with Vaska's compound suggests also that this phospholene ligand may not be readily deformed from the all-trans planar geometry exhibited by II.

Acknowledgment. We thank the Natural Sciences and Engineering Research Council of Canada for financial support.

Registry No. I, 110718-07-5; II, 110718-08-6; L, 2546-25-0; $[Pt(PEt_3)_4]$, 33937-26-7; $[Pt(\eta^2\text{-}C_2H_4)(PPh_3)_2]$, 12120-15-9.

Supplementary Material Available: Listings of anisotropic thermal parameters (Table IX), rms thermal vibrations (Table X), all bond distances (Table XI), all bond angles (Table XII), and torsional angles (Table XIII) (9 pages); a listing of calculated and observed structure factors (Table XIV) (54 pages). Ordering information is given on any current masthead page.

(37) Baddley, W. H. *J. Am. Chem. Soc.* **1966**, *88*, 4545.

Contribution from the Department of Chemistry, State University of New York at Albany, Albany, New York 12222

Derivatized Polyoxomolybdates. Synthesis and Characterization of Oxomolybdate Clusters Containing Coordinatively Bound Diazenido Units. Crystal and Molecular Structure of the Octanuclear Oxomolybdate $(NHEt_3)_2(n\text{-}Bu_4N)_2[Mo_8O_{20}(NNPh)_6]$ and Comparison to the Structures of the Parent Oxomolybdate $\alpha\text{-}(n\text{-}Bu_4N)_4[Mo_8O_{26}]$ and the Tetranuclear (Diazenido)oxomolybdates $(n\text{-}Bu_4N)_2[Mo_4O_{10}(OMe)_2(NNPh)_2]$ and $(n\text{-}Bu_4N)_2[Mo_4O_8(OMe)_2(NNC_6H_4NO_2)_4]$

Tze-Chen Hsieh, Shahid N. Shaikh, and Jon Zubieta*

Received April 24, 1987

Reactions of $\alpha\text{-}(n\text{-}Bu_4N)_4[Mo_8O_{26}]$ with phenylhydrazine yield a variety of derivatized polyoxomolybdates containing the *cis*-bis(diazenido)molybdenum core $[Mo(NNPh)_2]^{2+}$. When the reaction is carried out in methanol with excess (*p*-nitrophenyl)-hydrazine, $(n\text{-}Bu_4N)_2[Mo_4O_8(OMe)_2(NNAr)_4]$ is the major product. The tetranuclear polyoxomolybdate unit consists of the $[Mo_2(\mu\text{-}OMe)_2(NNAr)_4]^{2+}$ core, bridged by two doubly bridging bidentate $[MoO_4]^{2-}$ moieties. On the other hand, when the molybdate is present in excess, the unsymmetrically substituted tetranuclear cluster $(n\text{-}Bu_4N)_2[Mo_4O_{10}(OMe)_2(NNPh)_2]$ is isolated. This species is structurally analogous to $[Mo_4O_8(OMe)_2(NNPh)_4]^{2-}$, presenting the $[Mo_2O_2(\mu\text{-}OMe)_2(NNPh)_2]^{2+}$ core, and is characterized by a *cis*-$[MoO_2]^{2+}$ unit and a single *cis*-$[Mo(NNPh)_2]^{2+}$ unit, bridged by two methoxy groups. The tetranuclear unit is completed by the doubly bridging $[MoO_4]^{2-}$ units. In contrast, reactions of phenylhydrazine and NEt_3 with $\alpha\text{-}(n\text{-}Bu_4N)_4[Mo_8O_{26}]$ in acetonitrile yield the octanuclear polyoxomolybdate $(NHEt_3)_2(n\text{-}Bu_4N)_2[Mo_8O_{20}(NNPh)_6]$. The structure is related to that of the $\alpha\text{-}[Mo_8O_{26}]^{4-}$ parent polyoxomolybdate, by substitution of the two terminal oxo groups on each of three alternate molybdenum centers in the Mo_6O_6 crown and rotation of the pole-capping $[MoO_4]^{2-}$ units by ca. 45°, so as to engage three doubly bridging Mo_2O interactions per unit rather than three triply bridging Mo_3O interactions. The ^{17}O NMR spectra of the derivatized species are consistent with the solid-state structures, exhibiting resonances in the regions assigned to doubly bridging Mo_2O groups (400–520 ppm) and to terminal MoO groups (700–950 ppm). Crystal data are as follows. $\alpha\text{-}(n\text{-}Bu_4N)_4[Mo_8O_{26}]$: monoclinic space group $P2_1/n$, with a = 15.093 (3) Å, b = 16.011 (3) Å, c = 18.519 (4) Å, β = 91.36 (1)°, V = 4473.9 (3) Å^3, and Z = 2. Structure solution based on 3274 reflections converged at R = 0.039. $(n\text{-}Bu_4N)_2[Mo_4O_8(OMe)_2(NNC_6H_4\text{-}p\text{-}NO_2)_4]$: monoclinic space group $P2_1/n$, with a = 15.723 (2) Å, b = 14.058 (2) Å, c = 16.607 (3) Å, β = 95.28 (1)°, V = 3655.1 (2) Å^3, and Z = 2. Structure solution and refinement based on 2988 reflections converged at R = 0.063. $(n\text{-}Bu_4N)_2[Mo_4O_{10}(OMe)_2(NNPh)_2]$: monoclinic space group $C2/c$, with a = 15.472 (2) Å, b = 20.516 (3) Å, c = 19.077 (2) Å, β = 91.23 (1)°, V = 6054.1 (2), and Z = 4. Structure solution and refinement based on 1670 reflections converged at R = 0.066. $(NHEt_3)_2(n\text{-}Bu_4N)_2[Mo_8O_{20}(NNPh)_6]$: $P2_1/c$ with a = 18.495 (3) Å, b = 26.783 (5) Å, c = 21.470 (4) Å, β = 95.57 (1)°, V = 10585.0 (9) Å^3, and Z = 4; 6525 reflections, R = 0.051.

The polyoxoanions of molybdenum and tungsten have attracted continuing interest as catalysts, as spectroanalytical reagents, as imaging agents for electron microscopy, and as catalysts in the photooxidation of organic compounds.[1,2] Although the perceived analogies of the isopolymolybdate anions to metal oxide surfaces provide a current focus of attention, relatively few examples of organic derivatives of isopolymolybdates have been reported.[3-6] The coordination chemistry of the isopolymolybdates had been limited to the formylated derivative $[(HCO)_2Mo_8O_{28}]^{6-}$, the methoxy derivative $[Mo_8O_{24}(OCH_3)_4]^{4-}$, species formally incorporating an acetal group $[CH_2Mo_4O_{15}H]^{3-}$ and the related formylated methylenedioxomolybdate–formate cluster $[HCCHMo_4O_{17}CH]^{3-}$, and the pyridine-coordinated complex $[(C_5H_5N)_2Mo_8O_{26}]^{4-}$.[3-6] In each of these examples, the molybdenum centers are pseudooctahedrally coordinated either to six oxygen donors or, in the case of the pyridine-coordinated centers of $[(C_5H_5N)_2Mo_8O_{26}]^{4-}$, to five oxygen donors and a single pyridyl nitrogen.

We have recently demonstrated that the derivative chemistry of the isopolymolybdates may be extended to the organodiazenido group, –NNR,[7-9] and to the organohydrazido unit, –NNRR′,[10]

(1) Pope, M. T. *Heteropoly and Isopoly Oxometalates*; Springer-Verlag: New York, 1983.
(2) Ioannidis, I.; Papaconstantinou, E. *Inorg. Chem.* **1985**, *24*, 439. Hill, C. L.; Renneke, R. *J. Am. Chem. Soc.* **1986**, *108*, 3528.
(3) Adams, R. D.; Klemperer, W. G.; Liu, R.-S. *J. Chem. Soc., Chem. Commun.* **1979**, 256.
(4) McCarron, E. M., III; Harlow, R. L. *J. Am. Chem. Soc.* **1983**, *105*, 6179.
(5) Day, V. W.; Frederick, M. F.; Klemperer, W. G.; Liu, R.-S. *J. Am. Chem. Soc.* **1979**, *101*, 491; Day, V. W.; Thompson, M. R.; Day, C. S.; Klemperer, W. G.; Liu, R.-S. *J. Am. Chem. Soc.* **1980**, *102*, 5973.
(6) McCarron, E. M., III; Whitney, J. F.; Chase, D. B. *Inorg. Chem.* **1984**, *23*, 3276.
(7) Hsieh, T.-C.; Zubieta, J. *Inorg. Chem.* **1985**, *24*, 1287.
(8) Hsieh, T.-C.; Zubieta, J. *Polyhedron* **1986**, *5*, 305.
(9) Hsieh, T.-C.; Zubieta, J. *Polyhedron* **1986**, *5*, 1655.
(10) Shaikh, S. N.; Zubieta, J. *Inorg. Chem.* **1986**, *25*, 4613.

0020-1669/87/1326-4079$01.50/0

ligands that form robust complexes with molybdenum, displacing oxo groups via condensation type reactions. In contrast to the previously reported derivatives of isopolymolybdates, these latter complexes present both octahedral and tetrahedral molybdenum centers in the tetranuclear cores of general types $[Mo_4O_8(OR)_2(NNR)_4]^{2-}$ and $[Mo_4O_{10}(OR)_2(NNR_2)_2]^{2-}$. Since the synthesis of these organohydrazine derivatives of the isopolymolybdates is largely solvent dependent, the reaction chemistry of phenylhydrazine with $(NR_4)_4[Mo_8O_{26}]$ in non-alcoholic organic solvents, such as CH_2iCl_2 and MeCN, was investigated, resulting in the isolation of the octanuclear species $(HNEt_3)_2(n\text{-}Bu_4N)_2[Mo_8O_{20}(NNPh)_6]$.[11] In this paper, we report the synthesis, structure, ^{17}O NMR spectrum, and other spectroscopic characteristics of $(HNEt_3)_2(n\text{-}Bu_4N)_2[Mo_8O_{20}(NNPh)_6]$ and compare the structural characteristics to those of the parent isopolymolybdate $\alpha\text{-}(Bu_4N)_4[Mo_8O_{26}]$ and to those of the tetranuclear cluster $(n\text{-}Bu_4N)_2[Mo_4O_{10}(OMe)_2(NNPh)_2]$, which we synthesized in the course of the investigation.

Experimental Section

All chemicals were obtained from either Aldrich, Alfa, or Eastman. The parent isopolymolybdate, $\alpha\text{-}(\#\text{-}Bu_4N)_4[Mo_8O_{26}]$, was prepared by the literature method.[12] All manipulations were carried out under purified N_2 by using standard Schlenk techniques. Methanol and methylene chloride were dried over magnesium methoxide and CaH_2, respectively. Ethanol and acetonitrile were dried over magnesium ethoxide and CaH_2, respectively. Anhydrous ether and phenylhydrazine were passed through activated alumina prior to use. Elemental analyses were performed by Desert Analytics, Tuscon, AZ. The instrumentation used to obtain electronic and infrared spectra and X-ray diffraction data have been described previously.[13]

Synthesis of $(HNEt_3)_2(n\text{-}Bu_4N)_2[Mo_8O_{20}(NNPh)_6]$. Method 1. Addition of a mixture of phenylhydrazine (2.0 mL, 18.5 mmol) and NEt_3 (3.0 mL, 20.0 mmol) to a solution of $\alpha\text{-}[n\text{-}Bu_4N]_4[Mo_8O_{26}]$ (2.1 g, 1.0 mmol) in 50 mL of ethanol immediately produced an intensely colored purple solution. After being refluxed for 4 h, the solution was cooled to room temperature and 50 mL of diethylether was added. When the solution was cooled at 0 °C for 2 weeks, lustrous dark crystals of hexagonal habit were isolated. The yield of crystalline $(HNEt_3)_2(n\text{-}Bu_4N)_2[Mo_8O_{20}(NNPh)_6]$ was 0.24 g (10% based on Mo). A copious quantity of irregularly shaped purple-black crystals of $(n\text{-}Bu_4N)_2[Mo_4O_8(OEt)_2(NNPh)_4]$ grew from the filtrate upon standing. (0.80 g, 32% based on Mo). Anal. Calcd for $C_{80}H_{134}N_{16}O_{20}Mo_8$: C, 39.9; H, 5.61; N, 9.52. Found: C, 39.7; H, 5.40; N, 9.52. Electronic spectrum (λ_{max}, nm (ϵ, M^{-1} cm^{-1})): 530 (7.62×10^3), 304 (1.26×10^5). Infrared spectrum (KBr pellet, cm^{-1}): 2995 (m), 2990 (sh), 1622 (m), 1570 (s), 1490 (s), 1402 (m), 1250 (m), 890 (s), 810 (s), 790 (m), 760 (m), 730 (m). Conductivity (Λ, cm^2 mol^{-1} Ω^{-1} in 10^{-4} M solution in acetonitrile): 567 (4:1 electrolyte).

Method 2. The yield of the octanuclear species may be improved by using non-alcoholic solvents, in an atmosphere of dry N_2. A solution of phenylhydrazine (2.0 mL, 18.5 mmol) and NEt_3 (3.0 mL, 20.0 mmol) in 10 mL of acetonitrile was added to a refluxing solution of $\alpha\text{-}(n\text{-}Bu_4N)_4[Mo_8O_{26}]$ (2.1 g, 1.0 mmol) in 30 mL of acetonitrile. After the intensely colored purple solution was refluxed for 6 h, the solution was cooled to room temperature and the solvent stripped under vacuum at 25 °C. The purple oil thus obtained was washed with anhydrous diethyl ether and dissolved in 20 mL of hot acetonitrile. Upon addition of 40 mL of diethyl ether and storage at 0 °C for 10 days, crystalline $(n\text{-}Bu_4N)_4[Mo_8O_{20}(NNPh)_6]$ in 1.7 g yield (63.3%) was isolated. Anal. Calcd for $C_{100}H_{174}N_{16}O_{20}Mo_8$: C, 44.7; H, 6.52; N, 8.34. Found: C, 45.2; H, 6.42; N, 8.53.

Synthesis of $(n\text{-}Bu_4N)_2[Mo_4O_8(OMe)_2(NNC_6H_4\text{-}p\text{-}NO_2)_4]$. (Nitrophenyl)hydrazine (7.5 g, 0.05 mol) was added to a solution of $\alpha\text{-}(n\text{-}Bu_4N)_4[Mo_8O_{26}]$ (2.1 g, 1.0 mmol) in 20 mL of MeOH. After being refluxed for 2 h, the intensely colored purple solution was cooled to room temperature and diethyl ether was carefully layered over the methanolic solution. After the solution was allowed to stand for 2 weeks, lustrous purple-red crystals formed on the sides of the reaction flask. Yield: 0.72 g (30% based on Mo precursor). Anal. Calcd for $C_{58}H_{94}N_{14}O_{18}Mo_4$: C, 42.0; H, 5.71; N, 11.8. Found: C, 41.8; H, 5.76; N, 11.6. Electronic spectrum (λ_{max}, nm (ϵ, M^{-1} cm^{-1})): 520 (5.5×10^3), 407 (sh), 304 (2.7×10^4), 272 (2.8×10^4). IR (KBr pellet, cm^{-1}): 2990 (s), 2981 (sh), 1605 (m), 1565 (m), 1510 (s), 1487 (s), 1402 (m), 1245 (m), 902 (ms), 861 (ms), 793 (s), 730 (m).

Synthesis of $(n\text{-}Bu_4N)_2[Mo_4O_{10}(OMe)_2(NNPh)_2]$. Method 1. $(n\text{-}Bu_4N)_2[Mo_4O_{10}(OMe)_2(NNPh_2)_2]$[10] (0.5 g, 0.344 mmol) was placed in a Schlenk flask, and a solution of phenylhydrazine (0.11 g, 1.03 mmol) in 20 mL of a 1:1 v/v CH_2Cl_2–CH_3OH mixture was added. After 10 min of stirring, the color of the solution changed from orange to light red. Continued stirring for 16 h at room temperature produced an intensely colored violet solution. Careful layering of 30 mL of a 1:1 v/v dried pentane–ether mixture was followed by cooling for 4 weeks at 4 °C, resulting in lustrous violet crystals. The crystals were collected by filtration, washed with pentane, and vacuum dried. Yield: 0.26 g (58%). Anal. Calcd for $C_{46}H_{88}N_6O_{12}Mo_4$: C, 42.5; H, 6.82; N, 6.46. Found: C, 42.2; H, 6.51; N, 6.99. IR (KBr pellet, cm^{-1}): 2950 (s), 1590 (m), 1565 (m), 1465 (s), 1360 (s), 890 (s), 560 (m). Electronic spectrum (λ_{max}, nm, (ϵ, M^{-1} cm^{-1})): 525 (2.45×10^3), 304 (4.15×10^4), 275 (4.22×10^3).

Method 2. Phenylhydrazine (0.22 g, 2.03 mmol) was added to a solution of $\alpha\text{-}(n\text{-}Bu_4N)_4[Mo_8O_{26}]$ (1.08 g, 0.5 mmol) in 20 mL of methanol. After being refluxed for 12 h, the resultant purple solution was concentrated to 10 mL and layered with 25 mL of ether. After 3 weeks at 4 °C, lustrous violet crystals formed on the walls of the reaction flask. The crystals were collected and washed with pentane and ether. Yield: 0.31 g (24%).

^{17}O Nuclear Magnetic Resonance Spectra. (A) Sample Preparation. Samples were prepared by using 50% ^{17}O enriched water, purchased from Cambridge Chemicals. All preparative procedures involving ^{17}O-enriched water were carried out in closed systems in order to prevent isotopic dilution by atmospheric water. The ^{17}O-enriched sample of $\alpha\text{-}(n\text{-}Bu_4N)_4[Mo_8O_{26}]$ was prepared by the literature method of Klemperer.[14] ^{17}O-Enriched samples of the phenyldiazenido-derived complexes were prepared by adjusting the conditions described above in order to minimize isotopic dilution by atmospheric oxygen. Preparations were generally carried out on a 0.50-g scale.

(B) Spectral Measurements. ^{17}O NMR spectra were recorded at 297 K at 40.66 MHz by using the pulse FT NMR technique on a Varian XL-300 spectrometer interfaced with a Motorola 68000 microprocessor computer. The spectra were digitized by using 1600, 4160, 6976, or 8000 data points depending on the acquisition times and spectral band widths employed. The pulse width used for a 90° pulse was 25 μs. Deuteriated dichloromethane and acetonitrile were employed as internal locks. Spectra were obtained by using a double-precision acquisition technique in cylindrical 10-mm-o.d. sample tubes (3.0-mL sample volume) and referenced to internal $H_2{}^{17}O$. Chemical shifts are reported in parts per million with positive values in the low-field direction relative to $H_2{}^{17}O$. All chemical shifts and line width data were reproducible within ±2% and ±5%, respectively.

(C) Spectral Parameters. The following abbreviations are used: cpd for compound, sol for solvent, [X] for molar concentration of X, NT for number of transients, AT for acquisition time in ms, SW for sweep width in Hz, TO for transmitter offset in Hz, and LB for exponential line broadening in Hz.

1. cpd = $[(n\text{-}C_4H_9)_4N]_2[Mo_4O_{10}(\mu\text{-}OCH_3)_2(N_2Ph_2)_2]$, sol = CD_3CN–CH_2Cl_2 (1:2), [X] = 1.44×10^{-2}, NT = 23 180, AT = 50, SW = 69 930, TO = 20 000, LB = 30.
2. cpd = $[(n\text{-}C_4H_9)_4N]_2[Mo_4O_{10}(\mu\text{-}OCH_3)_2(N_2Ph)_2]$, sol = CD_2Cl_2–CH_2Cl_2 (1:2), [X] = 2.67×10^{-2}, NT = 144 316, AT = 10, SW = 80 000, TO = 26 000, LB = 50.
3. cpd = $[(n\text{-}C_4H_9)_4N]_2[Mo_4O_8(\mu\text{-}OCH_3)_2(N_2Ar)_4]$, sol = CD_2Cl_2–CH_2Cl_2 (1:2), [X] = 2.57×10^{-2}, NT = 28 020, AT = 50, SW = 80 000, TO = 26 000, LB = 50.
4. cpd = $[(n\text{-}C_4H_9)_4N]_4[Mo_8O_{20}(N_2Ph)_6]$, sol = CD_3CN–CH_2Cl_2 (1:2), [X] = 1.33×10^{-2}, NT = 35 709, AT = 50, SW = 69 930, TO = 20 000, LB = 50.
5. cpd = $[(n\text{-}C_4H_9)_4N]_2[Mo_2O_7]$, sol = CD_3CN–CH_3CN (1:2), [X] = 4.22×10^{-2}, NT = 268, AT = 200, SW = 69 930, TO = 20 000, LB = 10.
6. cpd = $[(n\text{-}C_4H_9)_4N]_4[\alpha\text{-}Mo_8O_{26}]$, sol = CD_3CN–CH_3CN (1:2), [X] = 1.55×10^{-2}, NT = 38 684, AT = 50, SW = 69 930, TO = 20 000, LB = 10.

X-ray Crystallographic Studies. The details of the crystal data, data collection methods, and refinement procedures are given in Table III. Full details of the crystallographic methodologies may be found in ref 15. Atomic positional parameters for the various structures are given in Tables IV, VI, VIII, and X.

(11) Hsieh, T.-C.; Zubieta, J. *J. Chem. Soc., Chem. Commun.* **1985**, 1749.
(12) Day, V. W.; Frederick, M. F.; Klemperer, W. G.; Shum, W. *J. Am. Chem. Soc.* **1977**, *99*, 6146.
(13) Nicholson, T.; Zubieta, J. *Inorg. Chem.* **1987**, *26*, 2094.
(14) Filowitz, M.; Ho, R. K. C.; Klemperer, W. G.; Shum, W. *Inorg. Chem.* **1979**, *18*, 93.
(15) Bruce, A.; Corbin, J. L.; Dahlstrom, P. L.; Hyde, J. R.; Minelli, M.; Steifel, E. I.; Spence, J. T.; Zubieta, J. *Inorg. Chem.* **1982**, *21*, 917.

Table I. Comparison of Selected Infrared Absorptions and Electronic Spectral Parameters for Phenyldiazenido-Derivatized Polyoxomolybdates

complex	IR, cm^{-1}	electronic spectrum		
		λ_{max}, nm	$10^{-3}\epsilon$, M^{-1} cm^{-1}	$10^{-3}\epsilon/[Mo(NNPh)_2]$
$(n\text{-}Bu_4N)_2[Mo_4O_{10}(OMe)_2(NNPh)_2]$	1590, $\nu(N\text{–}N_{asym})$ 1565, $\nu(N\text{–}N_{sym})$ 890, $\nu(Mo\text{–}O_t)$ 780, $\nu(Mo\text{–}O_b)$	525	2.45	2.45
$(n\text{-}Bu_4N)_2[Mo_4O_8(OMe)_2(NNC_6H_4NO_2)_4]$	1605, $\nu(N\text{–}N_{asym})$ 1565, $\nu(N\text{–}N_{sym})$ 902, $\nu(Mo\text{–}O_t)$ 861, $\nu(Mo\text{–}O_t)$ 793, $\nu(Mo\text{–}O_b)$	520	5.50	2.75
$(HNEt_3)_2(n\text{-}Bu_4N)_2[Mo_8O_{20}(NNPh)_6]$	1622, $\nu(N\text{–}N_{asym})$ 1570, $\nu(N\text{–}N_{sym})$ 890, $\nu(Mo\text{–}O_t)$ 810, $\nu(Mo\text{–}O_t)$ 790, $\nu(Mo\text{–}O_b)$ 760, $\nu(Mo\text{–}O_b)$	530	7.62	2.54

Table II. 40.66-MHz ^{17}O NMR Data for Organonitrogen-Derivatized Polyoxomolybdate Anion Clusters and Representative Polyoxomolybdate Anions

compd	chem shift (assignt) [line width][a,b]
$[Mo_2O_7]^{2-}$	257 (O_b) [192], 723 (O_t) [73]
$\alpha\text{-}[Mo_8O_{26}]^{4-}$	403 (O_b) [338], 504 (O_b') [520], 779 (O_t) [220], 873 (O_t') [222]
$[Mo_4O_{10}(OMe)_2(NNPh)_2]^{2-}$	419 [974] and 450 (O_2, O_3) [746], 771 (O_1) [653], 808 (O_4) [314]
$[Mo_4O_8(OMe)_2(NNAr)_4]^{2-}$	439 (O_2) [574], 757 (O_1) [297]
$[Mo_4O_{10}(OMe)_2(NNPh_2)_2]^{2-}$	425 (O_2) [370], 782 (O_1) [175], 936 (O_3) [1024]
$[Mo_8O_{20}(NNPh)_6]^{4-}$	423 (O_2) [649], 504 (O_3) [410], 733 (O_1) [167], 744 (O_4) [120]

[a] Chemical shifts are downfield from $H_2{}^{17}O$ in ppm. All peak widths at half-height are given in Hz. Spectra are recorded at 297 K. No signals were observed for alkoxide oxygens (see also ref 29). [b] Oxygen assignments refer to the labeling schemes displayed for the idealized structures in Figure 2. For $\alpha\text{-}[Mo_8O_{26}]^{4-}$, the assignment is that of ref 14. O_b refers to the bridging oxygens of the Mo_6O_6 crown, O_b' to the bridging oxygens from the capping $[MoO_4]^{2-}$ units to the crown, O_t is the terminal oxygens associated with the six crown molybdenum centers, and O_t' to the terminal oxygens of the capping units.

The structural analysis of complex **4** presented a number of difficulties. Data were initially collected on the $(n\text{-}Bu_4N)^+$ salt, $(n\text{-}Bu_4N)_4[Mo_8O_{20}(NNPh)_6]$. A 25% decline in the intensities of the standards was observed during the course of data collection. In addition to this problem, the $(n\text{-}Bu_4N)^+$ cations were severely disordered, resulting in a structure that converged at $R = 0.106$ and exhibited generally low resolution. Attempts to prepare $(PPh_4)^+$, $(PMePh_3)^+$, or $(AsPh_4)^+$ salts of **1** proving unsuccessful, data were collected on the mixed salt $(HNEt_3)_2(n\text{-}Bu_4N)_2[Mo_8O_{20}(NNPh)_6]$. Once again crystal decomposition was observed over the course of data collection. Mounting the crystal in a capillary in the presence of the mother liquor and employing a fast scan technique reduced the degree of decomposition to some 7–10% over the period of data collection. Refinement of these data converged to 0.051 and produced a perfectly satisfactory molecular geometry for the anion. However, the high-angle data were of poor quality, resulting in an unacceptable spread in the C–C bond distances of the $(n\text{-}Bu_4N)^+$ cations and the phenyl rings.

As a final recourse, a crystal of **1** was carefully mounted under nitrogen in a quartz capillary, in contact with the mother liquor of recrystallization. Data were collected at −40 °C by employing a Neslab Instruments Cryocool CC-60 aircooled mechanical refrigeration system. Data were collected at slow scan speeds, 1–15° min^{-1} over a period of 8 days. No significant crystal decomposition was observed.

Due to the size of the problem (495 parameters, 8226 unique data), phenyl groups were treated as idealized hexagons in the refinement procedure, and hydrogen atom positions were not calculated and included in the refinement. The final difference Fourier map suggested some disorder of the $(n\text{-}Bu_4N)^+$ cation, as indicated by a number of residuals of electron density in the range 0.5–0.8 e/Å^3 in positions consistent with C atom locations. Since refinement models including these peaks and using partial populations produced no significant improvement in the residuals, the expedient of assigning the C positions to the largest peaks consistent with normal C–C distances was employed. Although this resulted in some exaggerated thermal parameters, this model appeared adequate. The final difference Fourier map exhibited excursions of electron density of ca. 0.5 e/Å^3 at a distance of 0.5–1.0 Å from the Mo(1), Mo(3), and Mo(5) locations, in addition to those associated with the disordered $(n\text{-}Bu_4N)^+$ cation.

The structure of **4** presented difficulties similar to those uncovered for **1**. Again, data were collected at −40 °C by using slow scan speeds. Disorder of the $(n\text{-}Bu_4N)^+$ cation was again observed, as evident from the exaggerated thermal parameters, some spread in the C–C distances, and a number of electron density residuals on the order of 0.7 e/Å^3 associated with the region of space occupied by the cation. Again, no attempt was made to resolve the disorder since the anion geometry appeared acceptable.

The disorder problems associated with these structures are particularly difficult to eliminate. The chemistry of isopolyoxomolybdate anions is exceedingly counterion dependent, and attempts to prepare derivative salts often fail or result in isolation of other aggregates.

Results and Discussion

Syntheses and Spectroscopic Properties. In methanolic solution, isopolymolybdate anions react to give a variety of oxo–methoxy species of hexavalent molybdenum, of which $[Mo_8O_{24}(OCH_3)_4]^{4-}$ constitutes the major product. The initial step of the synthesis of the diazenido derivatives in methanolic solution would appear to be the formation of an equilibrium mixture of oxo–methoxy species, which subsequently react with phenylhydrazine, with concomitant cluster dissociation and reaggregation to yield tetranuclear species $[Mo_4O_8(OMe)_2(NNPh)_4]^{2-}$. The reaction with phenylhydrazine may be viewed formally as a simple condensation reaction to yield H_2O and the Mo=N=NHR unit, but evidently some internal redox step, perhaps involving Mo—OH, is necessary to remove the remaining hydrogen atom.

In ethanolic solution, the reaction of $\alpha\text{-}[Mo_8O_{26}]^{4-}$ with phenylhydrazine yields the analogous ethoxy-bridged tetranuclear species $[Mo_4O_8(OEt)_2(NNPh)_4]^{2-}$ as the major product. However, the octanuclear species $[Mo_8O_{20}(NNPh)_6]^{4-}$ is also isolated as a minor product of the reaction in ethanol. If the initial step of the reaction involves formation of the oxo–alkoxy species $[Mo_8O_{24}(OEt)_4]^{4-}$, the isolation of two reaction products suggests that $[Mo_8O_{24}(OEt)_4]^{4-}$ may form less readily than the methoxy analogue $[Mo_8O_{24}(OCH_3)_4]^{4-}$. Although $[Mo_8O_{24}(OCH_3)_4]^{4-}$ is readily isolated from methanolic solutions of $\alpha\text{-}[Mo_8O_{26}]^{4-}$, we were unable to isolate $[Mo_8O_{24}(OEt)_4]^{4-}$ in analytically pure form from ethanolic solutions.

These observations suggested two possible synthetic routes for the isolation of the octanuclear species $[Mo_8O_{20}(NNPh)_6]^{4-}$ in significant yield: the use of non-alcoholic solvents or variation in the reagent stoichiometry in alcoholic solvents. The former approach provided a significantly improved synthesis for $[Mo_8O_{20}(NNPh)_6]^{4-}$, particularly with CH_3CN as solvent, although CH_2Cl_2 also proved useful. In the absence of NEt_3, yields are considerably reduced, suggesting that the base may be required to deprotonate the hydrazido(2−) intermediate, Mo=N=NHR, yielding the diazenido linkage Mo=N=NR. The diazenido-coordinated molybdenum centers are thus in a formally reduced state Mo(0), if the diazenido group is formally considered a +1

Table III. Summary of Experimental Details for the X-ray Diffraction Studies of $(HNEt_3)_2(n\text{-}Bu_4N)_2[Mo_8O_{20}(NNPh)_6]$ (**1**), $(n\text{-}Bu_4N)_4[Mo_8O_{26}]$ (**2**), $(n\text{-}Bu_4N)_2[Mo_4O_8(OMe)_2(NNC_6H_4NO_2)_4]$ (**3**), and $(n\text{-}Bu_4N)_2[Mo_4O_{10}(OMe)_2(NNPh)_2]$ (**4**)

	1	**2**	**3**	**4**
	(A) Crystal Parameters[a]			
temp, K	233	294	294	233
a, Å	18.495 (3)	15.093 (3)	15.723 (2)	15.472 (2)
b, Å	26.783 (5)	16.011 (3)	14.058 (2)	20.516 (3)
c, Å	21.470 (4)	18.519 (4)	16.607 (3)	19.077 (3)
α, deg	90.00	90.00	90.00	90.00
β, deg	95.57 (1)	91.36 (1)	95.28 (1)	91.23 (1)
γ, deg	90.00	90.00	90.00	90.00
V, Å^3	10585.0 (9)	4473.9 (3)	3655.1 (2)	6054.1 (2)
space group	$P2_1/c$	$P2_1/n$	$P2_1/n$	$C2/c$
Z	4	2	2	4
ρ_{calcd}, g cm^{-3}	1.515	1.602	1.513	1.432
	(B) Measurement of Intensity Data			
cryst shape and color	dark red, parallelepiped	colorless, translucent cube	purple needles	violet rhombus
cryst dimens, mm	0.41 × 0.53 × 0.42	0.31 × 0.30 × 0.32	0.23 × 0.42 × 0.21	0.32 × 0.40 × 0.36
instrument	Nicolet R3m diffractometer			
radiation	Mo Kα (λ = 0.71073 Å)			
scan mode	coupled θ(cryst)–2θ(counter)			
scan rate, deg/min	1–30	7–30	7–30	1–30
scan range, deg	$2.0 < 2\theta \leq 50$			
scan length, deg	from $2\theta(K\alpha_1)$ – 1.0 to $2\theta(K\alpha_2)$ + 1.0			
bkgd meas	stationary cryst, stationary counter, at the beginning and end of each 2θ scan, each for the time taken for the scan			
stds	3 collected every 197			
no. of reflcns collcd ($+h,+k,\pm l$)	11 660	6526	4237	3963
no. of reflcns used in soln	8226, $F_o \geq 2.33\sigma(F_o)$	3274, $F_o \geq 6\sigma(F_o)$	2988, $F_o \geq 6\sigma(F_o)$	3589, $F_o \geq 2.33\sigma(F_o)$
	(C) Reduction of Intensity Data and Summary of Structure Solution and Refinement[b]			
abs coeff, cm^{-1}	9.85	11.24	7.24	8.44
abs cor	applied to **1** and **4**; based on χ scans for 5 reflcns with χ over 90 or 270°			
T_{max}/T_{min}	1.08	1.11	1.21	1.05
structure soln	Patterson synthesis yielded the Mo position; all remaining non-hydrogen atoms located via standard Fourier techniques			
atom scattering factors[c]	neutral atomic scattering factors were used throughout the analysis			
anomalous dispersion[d]	applied to all non-hydrogen atoms			
final discrepancy factor[e]				
R	0.051	0.039	0.063	0.066
R_w	0.074	0.040	0.065	0.079
goodness of fit[f]	1.648	1.360	1.4217	1.583

[a] From a least-squares fitting of the setting angle of 25 reflections. [b] All calculations were performed on a Data General Nova 3 computer with 32K of 16-bit words using local versions of the Nicolet SHELXTL interactive crystallographic software package as described in: Sheldrick, G. M. *Nicolet SHELXTL Operations Manual*; Nicolet XRD Corp.: Cupertino, CA 1979. Data were corrected for background, attenuators, and Lorentz and polarization effects in the usual fashion. [c] Cromer, D. T.; Mann, J. B. *Acta Crystallog., Sect. A: Cryst. Phys., Diffr., Theor. Gen. Crystallogr.* **1968**, *24*, 321. [d] *International Tables for X-ray Crystallography*; Kynoch: Birmingham, England, 1962; Vol. III. [e] $R = \sum[|F_o| - |F_c|/\sum|F_o|]$. $R_w = [\sum w(|F_o| - |F_c|)^2/\sum w|F_o|^2]^{1/2}$. $w = 1/\delta^2(F_o) + g^*(F_o)$; $g = 0.005$. [f] GOF $= [\sum w(|F_o| - |F_c|)^2/(NO - NV)]^{1/2}$ where NO is the number of observations and NV is the number of variables.

ligand in analogy to the isoelectronic nitrosyl ligand NO.

Attempts to synthesize $[Mo_8O_{20}(NNPh)_6]^{4-}$ from methanolic solutions by varying the relative amounts of ligand did not prove useful to this end but rather resulted in the isolation of $[Mo_4O_{10}(OMe)_2(NNPh)_2]^{2-}$. While reactions of α-$[Mo_8O_{26}]^{4-}$ with large excesses of phenylhydrazine (10-fold excess or greater per Mo) in ethanol yield only the previously characterized $[Mo_4O_8(OR)_2(NNPh)_4]^{2-}$ species, reactions using a 2- or 3-fold excess of phenylhydrazine gave a mixture of the tetranuclear cluster and $[Mo_8O_{20}(NNPh)_6]^{4-}$ in low yield. In contrast, addition of a stoichiometric or smaller amount of phenylhydrazine relative to α-$[Mo_8O_{26}]^{4-}$ in methanol as solvent yielded various mixtures of $[Mo_4O_8(OCH_3)_2(NNPh)_4]^{2-}$ and $[Mo_4O_{10}(OCH_3)_2(NNPh)_2]^{2-}$. However, the unsymmetrically substituted derivative $[Mo_4O_{10}(OCH_3)_2(NNPh)_2]^{2-}$ may be synthesized in analytically pure form from the reaction of $[Mo_4O_{10}(OMe)_2(NNPh_2)_2]^{2-}$ with a stoichiometric amount of phenylhydrazine. This latter reaction is not a simple displacement process since considerable structural rearrangement and reaggregation is required to generate the unsymmetrically substituted bis(diazenido)molybdenum species $[[Mo(NNPh)_2(\mu\text{-}OMe)_2(MoO_2)][MoO_4]_2]^{2-}$ from the symmetrical oxohydrazido species $[[MoO(NNPh_2)]_2(\mu\text{-}OMe)_2[MoO_4]_2]^{2-}$.

Both $[Mo_8O_{20}(NNPh)_6]^{4-}$ and $[Mo_4O_{10}(OMe)_2(NNPh)_2]^{2-}$ react with excess phenylhydrazine in methanol to give $[Mo_4O_8(OMe)_2(NNPh)_4]^{2-}$ in quantitative yield. The $[Mo_8O_{20}(NNPh)_6]^{4-}$ cluster is unstable in acidic solution, such that refluxing in acidic ethanol yields $[Mo_2Cl_2(OEt)_2(HOEt)_2(NNPh)_4]$, a binuclear ethoxy-bridged species whose structure has been described.[16]

In common with $[Mo_4O_8(OMe)_2(NNPh)_4]^{2-}$, the infrared spectra of $[Mo_8O_{20}(NNPh)_6]^{4-}$ and $[Mo_4O_{10}(OMe)_2(NNPh)_2]^{2-}$ exhibit two bands in the 1560–1640-cm^{-1} region characteristic of the symmetric and antisymmetric stretching modes of the *cis*-bis(diazenido) grouping. In addition, these species display a complex pattern of bands in the 720–930-cm^{-1} range attributable to Mo–O modes. The relevant infrared data are presented in Table I while Figure 1 compares the 500–2000 cm^{-1} regions of the infrared spectra of the tetranuclear and octanuclear species.

In common with other *cis*-bis(diazenido)molybdenum complexes, the electronic spectra of $[Mo_8O_{20}(NNPh)_6]^{4-}$ and $[Mo_4O_{10}(OMe)_2(NNPh)_2]^{2-}$ are characterized by an intense absorption in the visible region, at ca. 510–530 nm, which obeys Beer's law. This band appears to be characteristic of the *cis*-bis(diazenido)molybdenum unit, and it is seen (Table I) that the value of the molar absorptivity is a direct function of the number of *cis*-bis(diazenido)molybdenum units. Thus, the molar absorptivity at ca. 520 nm associated with a *cis*-bis(diazenido)molybdenum moiety is ca. 2.6×10^3.

(16) Hsieh, T.-C.; Zubieta, J. *Inorg. Chim. Acta* **1987**, *127*, 231.

Table IV. Atom Coordinates ($\times 10^4$) and Temperature Factors ($Å^2 \times 10^3$) for $(HNEt_3)_2(n\text{-}Bu_4N)_2[Mo_8O_{20}(NNPh)_6]$

atom	x	y	z	U_{eq}[a]	atom	x	y	z	U_{eq}[a]
Mo(1)	7565 (1)	1065 (1)	2282 (1)	52 (1)*	C(35)	7045 (7)	5457 (7)	410 (8)	82 (7)
Mo(2)	9179 (1)	1873 (1)	2631 (1)	50 (1)*	C(36)	7623 (9)	5195 (9)	721 (8)	96 (9)
Mo(3)	9692 (1)	3220 (1)	2826 (1)	58 (1)*	C(41)	4382 (7)	1981 (7)	3333 (1)	64 (7)
Mo(4)	7919 (1)	3739 (1)	2454 (1)	51 (1)*	C(42)	4292 (7)	2451 (7)	3056 (11)	97 (10)
Mo(5)	5929 (1)	3437 (1)	2219 (1)	55 (1)*	C(43)	3634 (7)	2704 (7)	3065 (11)	76 (8)
Mo(6)	6182 (1)	2041 (1)	2386 (1)	53 (1)*	C(44)	3065 (7)	2486 (7)	3351 (11)	78 (8)
Mo(7)	7781 (1)	2556 (1)	3430 (1)	48 (1)*	C(45)	3155 (7)	2016 (7)	3627 (11)	99 (9)
Mo(8)	7726 (1)	2542 (1)	1553 (1)	49 (1)*	C(46)	3814 (7)	1764 (7)	3618 (11)	111 (12)
O(1)	7556 (2)	477 (3)	256 (3)	77 (4)	C(51)	4695 (9)	1847 (9)	971 (9)	88 (10)
O(2)	7347 (3)	949 (3)	1538 (3)	55 (4)	C(52)	4634 (8)	2361 (8)	1053 (9)	92 (9)
O(3)	9806 (2)	3449 (4)	3531 (2)	82 (4)	C(53)	4122 (9)	2633 (9)	672 (8)	84 (8)
O(4)	10451 (4)	3377 (4)	2499 (5)	75 (5)	C(54)	3670 (8)	2390 (9)	209 (9)	103 (10)
O(5)	5677 (5)	3642 (3)	1468 (3)	74 (3)	C(55)	3731 (9)	1876 (9)	127 (9)	88 (9)
O(6)	5329 (3)	3695 (3)	2678 (4)	68 (4)	C(56)	4244 (9)	1604 (8)	508 (8)	89 (8)
O(7)	7749 (4)	2598 (5)	4228 (5)	63 (5)	N(99)	9551 (7)	−7 (8)	2193 (7)	81 (9)
O(8)	7767 (5)	2520 (5)	747 (4)	67 (4)	C(61)	10394 (9)	1 (9)	2296 (9)	84 (9)
O(11)	8433 (2)	1319 (4)	2471 (4)	75 (4)	C(62)	10659 (9)	486 (10)	2603 (10)	93 (11)
O(12)	9594 (2)	2561 (4)	2787 (2)	78 (4)	C(63)	11522 (10)	514 (10)	2568 (10)	96 (11)
O(13)	8980 (2)	3542 (4)	2401 (2)	81 (4)	C(64)	11771 (10)	1007 (11)	2931 (11)	79 (12)
O(14)	6868 (4)	3668 (3)	2502 (3)	68 (4)	C(65)	9247 (12)	406 (12)	1700 (11)	85 (12)
O(15)	5870 (4)	2762 (4)	2274 (5)	80 (1)	C(66)	9624 (11)	354 (11)	1071 (13)	84 (12)
O(16)	6821 (5)	1422 (4)	2517 (4)	74 (4)	C(67)	9135 (12)	703 (12)	600 (11)	80 (12)
O(21)	8476 (4)	2266 (3)	1950 (3)	64 (3)	C(68)	9558 (9)	685 (9)	−51 (8)	91 (12)
O(22)	7964 (3)	3146 (3)	3130 (4)	63 (4)	C(69)	9195 (9)	85 (9)	2783 (8)	90 (12)
O(23)	6921 (2)	2363 (4)	3074 (2)	74 (4)	C(70)	9392 (8)	−262 (9)	3317 (9)	95 (10)
O(24)	8458 (4)	2128 (4)	3287 (5)	63 (4)	C(71)	8869 (11)	−119 (11)	3768 (13)	101 (10)
O(25)	7722 (2)	3171 (4)	1769 (4)	82 (5)	C(72)	9385 (3)	55 (3)	4256 (3)	129 (2)
O(26)	6920 (5)	2238 (4)	1733 (4)	67 (4)	C(73)	9345 (13)	−538 (9)	1895 (9)	85 (14)
N(1)	9783 (5)	1679 (4)	2068 (4)	57 (6)	C(74)	8483 (13)	−591 (11)	1765 (11)	97 (14)
N(2)	10193 (4)	1527 (6)	1665 (2)	72 (6)	C(75)	8398 (14)	−1090 (11)	1347 (14)	109 (15)
N(3)	9742 (2)	1573 (6)	3255 (5)	70 (5)	C(76)	7590 (7)	−1159 (5)	1410 (6)	117 (3)
N(4)	10083 (6)	1332 (5)	3683 (6)	77 (5)	N(98)	5566 (9)	73 (8)	2775 (8)	81 (10)
N(5)	8074 (6)	4203 (5)	3064 (6)	66 (5)	C(81)	4728 (12)	129 (13)	2693 (13)	76 (10)
N(6)	8298 (4)	4520 (5)	3484 (4)	77 (5)	C(82)	4503 (13)	632 (12)	2358 (12)	88 (14)
N(7)	7920 (7)	4203 (5)	1862 (7)	98 (6)	C(83)	3651 (13)	666 (13)	2389 (12)	84 (14)
N(8)	8089 (5)	4499 (6)	1437 (5)	75 (6)	C(84)	3371 (15)	1174 (14)	2011 (14)	94 (12)
N(9)	5522 (5)	1863 (6)	2921 (5)	66 (5)	C(85)	5954 (16)	481 (16)	3209 (12)	76 (13)
N(10)	5049 (4)	1707 (5)	3259 (4)	69 (4)	C(86)	5659 (16)	489 (16)	3861 (13)	91 (17)
N(11)	5585 (5)	1767 (4)	1764 (4)	57 (4)	C(87)	5948 (15)	829 (12)	4397 (12)	98 (14)
N(12)	5198 (5)	1548 (4)	1333 (5)	71 (4)	C(88)	6730 (16)	875 (15)	4268 (17)	118 (17)
C(1)	10852 (8)	1785 (7)	1592 (9)	78 (8)	C(89)	5706 (15)	−465 (13)	3063 (14)	65 (14)
C(2)	11039 (8)	2224 (7)	1918 (9)	88 (9)	C(90)	6494 (14)	−585 (14)	3162 (12)	89 (15)
C(3)	11693 (8)	2464 (7)	1835 (9)	84 (9)	C(91)	6538 (16)	−1139 (14)	3460 (14)	114 (17)
C(4)	12159 (8)	2265 (7)	1427 (9)	98 (8)	C(92)	7280 (18)	−1249 (16)	3342 (18)	146 (19)
C(5)	11972 (8)	1826 (7)	1101 (9)	96 (9)	C(93)	5896 (15)	139 (15)	2170 (15)	92 (15)
C(6)	11319 (8)	1586 (7)	1183 (9)	70 (8)	C(94)	5630 (16)	−287 (16)	1722 (17)	88 (16)
C(11)	10684 (9)	1612 (7)	4070 (9)	85 (7)	C(95)	5884 (15)	−158 (13)	1081 (15)	84 (18)
C(12)	10810 (9)	2110 (7)	3925 (9)	94 (8)	C(96)	5614 (2)	357 (2)	912 (2)	96 (1)
C(13)	11345 (9)	2381 (7)	4281 (9)	102 (9)	N(97)	6560 (15)	1991 (13)	9799 (15)	88 (17)
C(14)	11754 (9)	2154 (7)	4784 (9)	83 (7)	C(101)	6045 (15)	2281 (15)	10086 (15)	92 (17)
C(15)	11629 (9)	1656 (7)	4929 (9)	82 (9)	C(102)	5989 (17)	2846 (17)	9821 (19)	146 (21)
C(16)	11094 (9)	1385 (7)	4572 (9)	102 (9)	C(103)	6695 (14)	1555 (14)	10238 (14)	82 (17)
C(21)	7767 (8)	4756 (8)	3792 (10)	75 (8)	C(105)	6218 (17)	1795 (17)	9226 (17)	100 (18)
C(22)	7981 (8)	5124 (8)	4231 (10)	58 (7)	C(104)	7345 (15)	1283 (15)	10088 (17)	82 (18)
C(23)	7464 (8)	5363 (8)	4558 (10)	108 (10)	C(106)	5730 (18)	1370 (16)	9190 (18)	168 (19)
C(24)	6732 (8)	5232 (8)	4446 (10)	75 (9)	N(96)	8964 (15)	2052 (13)	5254 (15)	106 (15)
C(25)	6518 (8)	4864 (8)	4007 (10)	79 (8)	C(111)	9437 (16)	2338 (14)	4902 (16)	78 (17)
C(26)	7036 (8)	4626 (8)	3680 (10)	86 (7)	C(112)	9466 (16)	2911 (16)	5112 (17)	83 (14)
C(31)	7490 (8)	4777 (8)	1081 (9)	78 (8)	C(113)	8814 (15)	1608 (15)	4913 (15)	105 (18)
C(32)	6778 (7)	4622 (7)	1129 (9)	72 (7)	C(114)	8409 (19)	1283 (16)	5311 (19)	123 (19)
C(33)	6199 (7)	4884 (7)	818 (8)	100 (8)	C(115)	9435 (17)	1971 (17)	5804 (15)	100 (15)
C(34)	6333 (7)	5302 (7)	459 (8)	70 (7)	C(116)	9987 (21)	1586 (19)	5930 (20)	99 (21)

[a] an asterisk denotes the equivalent isotropic U defined as one-third of the trace of the orthogonalized U_{eq} tensor.

A fundamental characterization property of an oxomolybdate species is provided by the ^{17}O NMR spectrum, which yields structural information based on the general correlation between downfield chemical shift and oxygen π-bond order.[17] The ^{17}O NMR data for the complexes of this study are presented in Table II, and representative spectra are shown in Figure 2.

The ^{17}O NMR spectra of the complex polyanions display the anticipated overall patterns. Bridging oxo groups appear in the 250–520 ppm range, while terminal oxo groups lie within the 700–950 ppm range characteristic of Mo(VI)–oxo compounds.[18] The linear correlation that exists between M–O π-bond order and ^{17}O chemical shift has been interpreted in terms of increasing π-bond order augmenting the paramagnetic screening of the oxygen nucleus, resulting in a larger chemical shift relative to $H_2{}^{17}O$.[18] Although the correlation between ^{17}O chemical shifts and Mo–O distances is nonlinear in the 1.6–2.4 Å range,[19] a linear

(17) Klemperer, W. G. *Angew. Chem., Int. Ed. Engl.* **1978**, *17*, 246.

(18) Kidd, R. G. *Can. J. Chem.* **1967**, *45*, 605.

(19) Freeman, M. A.; Schultz, F. A.; Reilley, C. N. *Inorg. Chem.* **1982**, *21*, 567.

Table V. Selected Bond Lengths (Å) and Angles (deg) for $(HNEt_3)_2(n\text{-}Bu_4N)_2[Mo_8O_{20}(NNPh)_6]$

Mo(1)–O(1)	1.688 (4)	Mo(5)–O(5)	1.725 (3)
Mo(1)–O(2)	1.639 (3)	Mo(5)–O(6)	1.699 (3)
Mo(1)–O(11)	1.755 (3)	Mo(5)–O(14)	1.887 (2)
Mo(1)–O(16)	1.788 (3)	Mo(5)–O(15)	1.815 (3)
Mo(2)–O(11)	2.033 (3)	Mo(6)–O(15)	2.024 (3)
Mo(2)–O(12)	2.013 (3)	Mo(6)–O(16)	2.040 (3)
Mo(2)–O(21)	2.137 (3)	Mo(6)–O(23)	2.099 (3)
Mo(2)–O(24)	2.144 (3)	Mo(6)–O(26)	2.118 (2)
Mo(2)–N(1)	1.800 (3)	Mo(6)–N(9)	1.820 (3)
Mo(2)–N(3)	1.805 (3)	Mo(6)–N(11)	1.803 (3)
Mo(3)–O(3)	1.628 (4)	Mo(7)–O(7)	1.724 (3)
Mo(3)–O(4)	1.683 (4)	Mo(7)–O(22)	1.752 (3)
Mo(3)–O(12)	1.776 (4)	Mo(7)–O(23)	1.771 (3)
Mo(3)–O(13)	1.753 (4)	Mo(7)–O(24)	1.747 (4)
Mo(4)–O(13)	2.047 (3)	Mo(8)–O(8)	1.740 (3)
Mo(4)–O(14)	1.965 (2)	Mo(8)–O(21)	1.722 (2)
Mo(4)–O(22)	2.147 (3)	Mo(8)–O(25)	1.749 (3)
Mo(4)–O(25)	2.123 (3)	Mo(8)–O(26)	1.773 (3)
Mo(4)–N(5)	1.808 (3)		
Mo(4)–N(7)	1.777 (4)		
N(1)–N(2)	1.27 (1)	N(7)–N(8)	1.26 (1)
N(3)–N(4)	1.24 (1)	N(9)–N(10)	1.26 (1)
N(5)–N(6)	1.25 (1)	N(11)–N(12)	1.26 (1)
O(1)–Mo(1)–O(2)	99.4 (1)	O(5)–Mo(5)–O(6)	106.2 (6)
O(1)–Mo(1)–O(11)	108.6 (2)	O(5)–Mo(5)–O(14)	110.6 (7)
O(1)–Mo(1)–O(16)	111.3 (2)	O(5)–Mo(5)–O(15)	111.4 (1)
O(2)–Mo(1)–O(11)	115.6 (2)	O(6)–Mo(5)–O(14)	108.2 (2)
O(2)–Mo(1)–O(16)	104.7 (1)	O(6)–Mo(5)–O(15)	108.7 (3)
O(11)–Mo(1)–O(16)	116.1 (5)	O(14)–Mo(5)–O(15)	111.4 (2)
O(11)–Mo(2)–O(12)	159.8 (1)	O(15)–Mo(6)–O(16)	161.3 (2)
O(21)–Mo(2)–N(3)	175.1 (2)	O(23)–Mo(6)–N(11)	176.8 (3)
O(24)–Mo(2)–N(1)	178.1 (2)	O(26)–Mo(6)–N(9)	177.7 (2)
N(1)–Mo(2)–N(3)	91.2 (2)	N(9)–Mo(6)–N(11)	87.7 (2)
O(3)–Mo(3)–O(4)	104.8 (3)	O(7)–Mo(7)–O(22)	109.4 (2)
O(3)–Mo(3)–O(12)	114.9 (2)	O(7)–Mo(7)–O(23)	109.4 (2)
O(3)–Mo(3)–O(13)	108.8 (2)	O(7)–Mo(7)–O(24)	108.1 (2)
O(4)–Mo(3)–O(12)	108.3 (2)	O(22)–Mo(7)–O(23)	107.6 (1)
O(4)–Mo(3)–O(13)	106.0 (2)	O(22)–Mo(7)–O(24)	111.1 (3)
O(12)–Mo(3)–O(13)	113.3 (2)	O(23)–Mo(7)–O(24)	111.2 (3)
O(13)–Mo(4)–O(14)	159.5 (2)	O(8)–Mo(8)–O(21)	111.5 (2)
O(22)–Mo(4)–N(7)	175.9 (2)	O(8)–Mo(8)–O(25)	107.3 (2)
O(25)–Mo(4)–N(5)	177.4 (2)	O(21)–Mo(8)–O(26)	110.4 (2)
N(5)–Mo(4)–N(7)	91.5 (3)	O(21)–Mo(8)–O(25)	107.8 (2)
		O(21)–Mo(8)–O(26)	110.4 (2)
		O(25)–Mo(8)–O(26)	111.0 (3)

correlation exists in the narrower range of terminal Mo–O distances of 1.6–1.9 Å.[20] The rather broad widths at half-height for the ^{17}O signals are indicative of polynuclear species in solution.

A more detailed analysis may be attempted by comparing the ^{17}O NMR spectra of the various derivatized clusters to those of the parent anions. The tetranuclear species $(n\text{-}Bu_4N)_2[Mo_4O_8(OMe)_2(NNAr)_4]$, as shown by the schematic of Figure 2 and the structural discussion to follow, displays an equivalent set of terminal oxo groups O_1 and chemically equivalent bridging oxo groups O_2 with ^{17}O resonances at 757 and 439 ppm, respectively. On the other hand, the unsymmetrically substituted species $(n\text{-}Bu_4N)_2[Mo_4O_{10}(OMe)_2(NNPh)_2]$ possesses four nonequivalent types of oxo groups. The terminal oxo resonances at 808 and 771 ppm may be assigned to O_4 and O_1, respectively. A range of 730–790 ppm appears to be characteristic for terminal oxo groups of a bidentate $[MoO_4]^{2-}$ unit having two terminal oxo groups since $(n\text{-}Bu_4N)_4[Mo_8O_{26}]$, $(n\text{-}Bu_4N)_2[Mo_4O_8(OMe_2)(NNAr)_4]$, $(n\text{-}Bu_4N)_2[Mo_4O_{10}(OMe)_2(NNPh_2)_2]$, $(n\text{-}Bu_4N)_2[Mo_4O_{10}(OMe)_2(NNPh)_2]$, and $[Mo_8O_{20}(NNPh)_6]^{4-}$ all display resonances in this region assignable to this type of terminal oxo group. Although intensities of ^{17}O NMR resonances provide only a qualitative measure of the relative number of oxygen nuclei, the relative peak heights of the resonances as 771 and 808 ppm for $[Mo_4O_{10}(OMe)_2(NNPh)_2]^{2-}$ support the assignments of these resonances to O_1 and O_4, respectively. The X-ray data (vide infra) are of marginal significance in this instance but do support the assignment: the Mo–O_1 type interaction presents a distance of 1.672 (2) Å while the Mo–O_4 type bond is shorter, 1.661 (2) Å, in agreement with the general trends.

The nonequivalent bridging oxygens of $[Mo_4O_{10}(OMe)_2(NNPh)_2]^{2-}$ are also well resolved at 419 and 450 ppm. Since the average Mo–O bond distances for the O_2 and O_3 type bridging interactions are 1.906 (2) and 1.930 (2) Å, respectively, an unambiguous assignment can not be made on the basis of the bond lengths alone.

The structure of a third tetranuclear polyanion, $[Mo_4O_{10}(OMe)_2(NNPh_2)_2]^{2-}$, is shown schematically in Figure 2, illustrating the three nonequivalent oxo environments. In this instance, the resonance from the bridging oxo group O_2 may be assigned unambiguously to the absorption at 425 ppm, an assignment consistent with those for other examples of this type of bridging oxo group. The resonances at 782 and 936 ppm are assigned to O_1 and O_3, respectively. The 782 ppm resonance occurs in the range associated with *cis*-dioxo groups of a bidentate bridging

(20) Miller, K. F.; Wentworth, R. A. D. *Inorg. Chem.* **1979**, *18*, 984.

Table VI. Atom Coordinates ($\times 10^4$) and Temperature Factors ($Å^2 \times 10^3$) for $\alpha\text{-}(n\text{-}Bu_4N)_4[Mo_8O_{26}]$

atom	x	y	z	U_{eq}[a]
Mo(1)	4051 (1)	4269 (1)	−1 (1)	30 (1)*
Mo(2)	6435 (1)	3367 (1)	9 (1)	52 (1)*
Mo(3)	5702 (1)	4228 (1)	−1559 (1)	44 (1)*
Mo(4)	4283 (1)	5837 (1)	−1598 (1)	44 (1)*
O(1)	3213 (4)	3550 (4)	14 (3)	51 (2)*
O(2)	7491 (4)	3312 (4)	359 (4)	78 (3)*
O(3)	6232 (5)	2407 (4)	−302 (4)	79 (3)*
O(4)	5509 (4)	3248 (4)	−1876 (3)	70 (3)*
O(5)	6341 (4)	4668 (4)	−2191 (3)	66 (3)*
O(6)	3248 (4)	5850 (4)	−1962 (3)	67 (3)*
O(7)	4897 (4)	6336 (4)	−2225 (3)	65 (3)*
O(21)	5750 (4)	3345 (4)	870 (3)	53 (2)*
O(22)	6604 (4)	4006 (4)	−841 (3)	54 (2)*
O(23)	4553 (4)	4688 (4)	−1749 (3)	46 (2)*
O(31)	3701 (4)	5170 (4)	−475 (3)	52 (2)*
O(32)	5039 (4)	6170 (4)	457 (3)	50 (2)*
O(33)	4384 (4)	4516 (4)	911 (3)	47 (2)*
N(11)	7517 (5)	7047 (4)	2010 (4)	48 (2)
C(11)	7647 (6)	6220 (6)	1618 (5)	54 (3)
C(12)	8503 (7)	5755 (7)	1804 (6)	68 (3)
C(13)	8600 (8)	4976 (7)	1335 (6)	71 (3)
C(14)	8732 (7)	5168 (7)	565 (5)	74 (3)
C(15)	7548 (7)	6939 (7)	2824 (5)	63 (3)
C(16)	6847 (8)	6352 (7)	8111 (6)	75 (3)
C(17)	6950 (10)	6262 (9)	8946 (7)	101 (4)
C(18)	7768 (11)	5820 (11)	4166 (9)	169 (7)
C(19)	6619 (7)	7377 (6)	1736 (5)	56 (3)
C(20)	6355 (7)	8219 (7)	2037 (6)	72 (3)
C(21)	5534 (8)	8506 (9)	1610 (7)	102 (4)
C(22)	5172 (11)	9285 (9)	1866 (8)	127 (5)
C(23)	8260 (7)	7649 (7)	1834 (5)	60 (3)
C(24)	8329 (8)	7882 (8)	1058 (6)	89 (4)
C(25)	9072 (11)	8549 (11)	1022 (9)	133 (6)
C(26)	9095 (16)	8938 (15)	423 (11)	293 (14)
N(12)	2776 (5)	2510 (5)	2192 (4)	45 (2)
C(31)	3423 (7)	2459 (6)	1569 (5)	57 (3)
C(32)	3454 (8)	1650 (8)	1191 (7)	84 (4)
C(33)	4242 (10)	1643 (11)	692 (8)	119 (5)
C(34)	4485 (19)	1001 (14)	362 (15)	349 (19)
C(35)	2968 (6)	1858 (6)	2757 (5)	56 (3)
C(36)	3898 (7)	1867 (7)	3099 (6)	73 (3)
C(37)	3942 (8)	1263 (7)	3740 (5)	69 (3)
C(38)	3756 (8)	394 (7)	3547 (6)	82 (4)
C(39)	1844 (7)	2330 (7)	1915 (6)	62 (3)
C(40)	1457 (8)	2890 (7)	1333 (6)	80 (3)
C(41)	475 (8)	2616 (9)	1223 (7)	94 (4)
C(42)	39 (10)	3105 (10)	658 (7)	127 (5)
C(43)	2854 (7)	3378 (6)	2509 (5)	57 (3)
C(44)	2303 (8)	3549 (8)	3155 (7)	90 (4)
C(45)	2478 (9)	4390 (9)	3505 (8)	105 (4)
C(46)	3357 (10)	4451 (11)	3828 (8)	149 (6)

[a] An asterisk denotes the equivalent isotropic U defined as one-third of the trace of the orthogonalized U_{eq} tensor.

Table VII. Bond Lengths (Å) and Angles (deg) for $(n\text{-}Bu_4N)_4[Mo_8O_{26}]$

Mo(1)–O(1)	1.711 (6)	Mo(3)–O(22)	1.913 (6)
Mo(1)–O(31)	1.763 (6)	Mo(3)–O(23)	1.909 (5)
Mo(1)–O(32)	1.775 (6)	Mo(3)–O(32′)	2.454 (6)
Mo(1)–O(33)	1.796 (6)	Mo(3)–O(33′)	2.346 (6)
Mo(2)–O(2)	1.708 (6)	Mo(4)–O(6)	1.687 (6)
Mo(2)–O(3)	1.667 (7)	Mo(4)–O(7)	1.703 (6)
Mo(2)–O(21)	1.922 (6)	Mo(4)–O(31)	2.515 (6)
Mo(2)–O(22)	1.899 (2)	Mo(4)–O(31)	2.515 (6)
Mo(2)–O(31′)	2.506 (6)	Mo(4)–O(21′)	1.880 (6)
Mo(2)–O(32′)	2.481 (6)	Mo(4)–O(33′)	2.421 (6)
Mo(3)–O(5)	1.689 (6)		
O(1)–Mo(1)–O(31)	110.2 (3)	O(22)–Mo(3)–O(33′)	81.4 (2)
O(1)–Mo(1)–O(32)	108.8 (3)	O(23)–Mo(3)–O(32′)	79.8 (2)
O(1)–Mo(1)–O(33)	108.8 (3)	O(23)–Mo(3)–O(33)	81.4 (2)
O(31)–Mo(1)–O(32)	108.3 (3)	O(32′)–Mo(3)–O(33′)	76.4 (2)
O(31)–Mo(1)–O(33)	111.2 (3)	O(6)–Mo(4)–O(7)	103.6 (3)
O(32)–Mo(1)–O(33)	109.4 (3)	O(6)–Mo(4)–O(23)	98.7 (3)
O(2)–Mo(2)–O(3)	104.3 (3)	O(6)–Mo(4)–O(23)	89.8 (3)
O(2)–Mo(2)–O(3)	101.5 (3)	O(6)–Mo(4)–O(21′)	103.7 (3)
O(2)–Mo(2)–O(22)	101.5 (3)	O(6)–Mo(4)–O(33′)	164.4 (3)
O(2)–Mo(2)–O(31′)	90.3 (3)	O(7)–Mo(4)–O(23)	103.4 (2)
O(2)Mo(2)–O(32′)	165.5 (3)	O(7)–Mo(4)–O(31)	166.0 (2)
O(3)–Mo(2)–O(21)	99.9 (3)	O(7)–Mo(4)–O(21)	100.7 (3)
O(3)–Mo(2)–O(22)	103.7 (3)	O(7)–Mo(4)–O(31)	78.0 (2)
O(3)–Mo(2)–O(31′)	164.7 (3)	O(23)–Mo(4)–O(31)	78.0 (2)
O(3)–Mo(2)–O(32′)	89.9 (3)	O(23)–Mo(4)–O(21′)	141.9 (2)
O(21)–Mo(2)–O(32′)	141.5 (3)	O(23)–Mo(4)–O(33′)	71.0 (2)
O(21)–Mo(2)–O(31′)	71.4 (2)	O(31)–Mo(4)–O(21′)	71.8 (2)
O(21)–Mo(2)–O(32′)	78.4 (2)	O(31)–Mo(4)–O(33′)	76.7 (2)
O(22)–Mo(2)–O(31′)	78.2 (2)	O(21′)–Mo(4)–O(33′)	79.8 (2)
O(22)–Mo(2)–O(32′)	71.8 (2)	Mo(1)–O(31)–Mo(4)	130.7 (3)
O(31′)–Mo(2)–O(32′)	76.1 (2)	Mo(1)–O(31)–Mo(2)	128.3 (3)
O(4)–Mo(3)–O(5)	104.0 (3)	Mo(1)–O(32)–Mo(2′)	130.6 (3)
O(4)–Mo(3)–O(22)	100.5 (3)	Mo(1)–O(32)–Mo(3′)	132.2 (3)
O(4)–Mo(3)–O(23)	98.3 (3)	Mo(1)–O(33)–Mo(3)	130.7 (3)
O(4)–Mo(3)–O(32′)	88.3 (3)	Mo(1)–O(33)–Mo(4′)	130.8 (3)
O(4)–Mo(3)–O(33′)	163.3 (3)	Mo(2)–O(21)–Mo(4′)	127.3 (3)
(5)–Mo(3)–O(22)	98.7 (3)	Mo(2)–O(22)–Mo(3)	124.7 (3)
O(5)–Mo(3)–O(23)	104.0 (3)	Mo(3)–O(23)–Mo(4)	122.7 (3)
O(5)–Mo(3)–O(32′)	166.3 (3)	Mo(4)–O(31)–Mo(2′)	85.5 (2)
O(5)–Mo(3)–O(33′)	92.1 (3)	Mo(2′)–O(32)–Mo(3)	86.8 (2)
O(22)–Mo(3)–O(32′)	72.7 (2)	Mo(3′)–O(33)–Mo(4)	89.3 (2)

$[MoO_4]^{2-}$ unit. The O_3 type terminal oxo group is bonded to a molybdenum center having no other terminal oxo unit and may be anticipated to participate more effectively in π-bonding, shifting the resonance downfield.

Inspection of the schematic for the structure of $[Mo_8O_{20}(NNPh)_6]^{4-}$ reveals four nonequivalent oxygen environments. The resonances at 423 and 504 ppm are assigned to the bridging oxo groups O_2 and O_3, respectively. The O_2 resonance is assigned on the basis of comparison to other structures exhibiting bidentate bridging $[MoO_4]^{2-}$ units, for which the bridging oxo resonances appear in the 400–450 ppm range. The O_3 type bridging oxo group is then associated with the 504 ppm resonance. These assignments are consistent with the structural data that present Mo_{oct}-O bond distances of ca. 1.80 and 2.13 Å for Mo–O_3 and Mo–O_2 bond types, respectively. The terminal oxo resonance cannot be assigned unambiguously, although the conventional arguments would predict that the 744 ppm resonance be associated with O_4.

Description of the Structures. The structure of the $[Mo_8O_{20}(NNPh)_6]^{4-}$ complex anion is displayed in Figure 3, atomic positional parameters are given in Table IV and relevant bond lengths and angles in Table V. The anion crystallizes as discrete octanuclear units incorporating coordinatively bound phenyldiazenido groups. The overall geometry may be described in terms of an equatorial girdle of six oxo-bridged molybdenum centers, alternating tetraoxomolybdate centers $[MoO_4]^{2-}$, and *cis*-bis(diazenido) moieties $[Mo(NNPh)_2]^{2+}$, with tripodal $[MoO_4]^{2-}$ tetrahedra capping the poles. Alternatively, the structure may be viewed in terms of the polyhedron model shown in Figure 5, illustrating that the irregular ring consists of alternating octahedra $[MoO_4N_2]$ and tetrahedra $[MoO_4]$ linked by corner-shared

Table VIII. Atom Coordinates ($\times 10^4$) and Temperature Factors ($Å^2 \times 10^3$) for $(n\text{-}Bu_4N)_2[Mo_4O_8(\mu\text{-}OCH_3)_2(N_2C_6H_4NO_2)_4]$

atom	x	y	z	U_{iso}[a]
Mo(1)	4946 (1)	3770 (1)	97 (1)	34 (1)*
Mo(2)	5770 (1)	5136 (1)	1698 (1)	43 (1)*
O(1)	6731 (5)	5155 (5)	2285 (4)	81 (3)*
O(2)	4972 (5)	5227 (5)	2311 (4)	85 (3)*
O(11)	5764 (4)	6116 (4)	1002 (3)	38 (2)*
O(12)	5679 (4)	4014 (4)	1153 (3)	44 (2)*
O(21)	4353 (3)	5079 (4)	377 (3)	37 (2)*
Cm	3490 (6)	5172 (7)	604 (6)	56 (4)*
N(1)	4199 (5)	2977 (5)	541 (4)	41 (3)*
N(2)	3641 (5)	2486 (5)	815 (4)	51 (3)*
N(3)	5624 (5)	2818 (5)	−202 (4)	42 (2)
N(4)	6170 (5)	2247 (6)	−398 (5)	58 (2)
C(1)	3692 (6)	2371 (7)	1659 (5)	49 (3)
C(2)	4228 (7)	2884 (7)	2199 (6)	58 (3)
C(3)	4248 (7)	2739 (8)	3022 (7)	70 (3)
C(4)	3741 (7)	2071 (7)	3298 (6)	59 (3)
C(5)	3201 (8)	1543 (9)	2792 (7)	85 (4)
C(6)	3164 (7)	1713 (8)	1967 (7)	80 (4)
N(11)	3788 (8)	1894 (8)	4171 (7)	106 (4)
O(31)	4375 (8)	2298 (8)	4596 (7)	145 (4)
O(32)	3287 (8)	1399 (9)	4415 (7)	171 (5)
C(11)	6174 (6)	2014 (7)	−1225 (6)	56 (3)
C(12)	5664 (7)	2427 (8)	−1825 (6)	65 (3)
C(13)	5723 (7)	2233 (7)	−2631 (6)	64 (3)
C(14)	6314 (7)	1875 (8)	−2806 (7)	69 (3)
C(15)	6817 (8)	1137 (9)	−2233 (7)	88 (4)
C(16)	6770 (7)	1340 (8)	−1423 (7)	83 (4)
N(12)	6428 (8)	1385 (9)	−3665 (7)	108 (4)
O(33)	6023 (7)	1850 (8)	−4146 (7)	132 (4)
O(34)	6861 (8)	683 (9)	−3773 (7)	166 (5)
N(99)	7663 (5)	7986 (5)	1401 (4)	46 (2)
C(41)	7798 (6)	7974 (7)	2320 (5)	57 (3)
C(42)	7210 (7)	7365 (8)	2736 (6)	69 (3)
C(43)	7380 (7)	7416 (8)	3640 (6)	79 (4)
C(44)	6841 (9)	6739 (10)	4073 (8)	111 (5)
C(45)	6787 (6)	8320 (7)	1122 (6)	49 (3)
C(46)	6538 (7)	9283 (7)	1420 (6)	62 (3)
C(47)	5734 (8)	9651 (8)	1000 (7)	89 (4)
C(48)	5407 (8)	10564 (9)	1282 (8)	103 (5)
C(49)	8334 (6)	8633 (7)	1100 (6)	57 (3)
C(50)	8251 (6)	8812 (8)	197 (6)	63 (3)
C(51)	9018 (7)	9330 (8)	−61 (7)	76 (3)
C(52)	8916 (8)	9588 (9)	−956 (7)	97 (4)
C(53)	7748 (6)	6986 (7)	1075 (6)	51 (3)
C(54)	8596 (7)	6477 (7)	1269 (6)	64 (3)
C(55)	8566 (7)	5458 (7)	1000 (7)	70 (3)
C(56)	9392 (8)	4943 (9)	1162 (8)	98 (4)

[a] An asterisk denotes the equivalent isotropic U defined as one-third of the trace of the orthogonalized U_{iso} tensor.

Table IX. Bond Lengths (Å) and Angles (deg) for $(n\text{-}Bu_4N)_2[Mo_4O_8(OMe)_2(NNC_6H_4NO_2)_4]$

Mo(1)–N(1)	1.823 (8)	Mo(2)–O(2)	1.691 (8)
Mo(1)–N(3)	1.809 (7)	Mo(2)–O(11)	1.798 (5)
Mo(1)–O(21)	2.133 (5)	Mo(2)–O(12)	1.818 (5)
Mo(1)–O(21′)	2.148 (5)	N(1)–N(2)	1.235 (11)
Mo(1)–O(11′)	2.057 (5)	N(2)–O(1)	1.406 (11)
Mo(1)–O(12)	2.036 (5)	N(3)–N(4)	1.240 (11)
Mo(2)–O(1)	1.721 (7)	N(4)–C(11)	1.412 (12)
N(1)–Mo(1)–N(3)	94.4 (3)	O(21)–Mo(1)–O(12)	83.7 (2)
N(1)–Mo(1)–O(21)	97.4 (3)	O(21′)–Mo(1)–O(11′)	82.6 (2)
N(1)–Mo(1)–O(21′)	168.6 (3)	O(21′)–Mo(1)–O(12)	85.4 (2)
N(1)–Mo(1)–O(11′)	95.1 (3)	O(11′)–Mo(1)–O(12)	165.7 (2)
N(1)–Mo(1)–O(12)	95.1 (3)	Mo(1)–N(1)–N(2)	174.9 (7)
N(3)–Mo(1)–O(21)	168.1 (3)	Mo(1)–N(3)–N(4)	172.1 (7)
N(3)–Mo(1)–O(11′)	97.0 (3)	N(1)–N(2)–C(1)	117.0 (7)
N(3)–Mo(1)–O(11′)	95.7 (3)	N(3)–N(4)–C(11)	118.0 (8)
N(3)–Mo(1)–O(12)	93.5 (3)	Mo(1)–O(21)–Mo(1′)	108.7 (2)
O(21)–Mo(1)–O(21′)	71.3 (2)	Mo(1)–O(12)–Mo(2)	126.0 (3)
O(21)–Mo(1)–O(11′)	85.1 (2)		

contacts and capped above and below by $[MoO_4]$ tetrahedra, sharing three corners. The structure thus approximates D_{3h} symmetry, with the 3-fold axis passing through Mo(7), O(7),

Table X. Atom Coordinates ($\times 10^4$) and Temperature Factors ($Å^2 \times 10^3$) for $(n\text{-}Bu_4N)_2[Mo_4O_{10}(OMe)_2(NNPh)_2]$

atom	x	y	z	U_{eq}[a]
Mo(1)	3274 (1)	1559 (1)	1908 (1)	60 (1)*
Mo(2)	5000	644 (1)	2500	46 (1)*
Mo(3)	5000	2424 (1)	2500	36 (1)*
O(1)	3701 (1)	2299 (1)	2293 (1)	71 (1)*
O(2)	3765 (1)	826 (1)	2317 (1)	81 (1)*
O(3)	2221 (1)	1537 (1)	2086 (1)	72 (1)*
O(4)	3347 (2)	1567 (1)	1014 (1)	84 (1)*
O(5)	4840 (1)	165 (1)	3170 (1)	82 (1)*
O(6)	5065 (1)	1565 (1)	1861 (1)	69 (1)*
N(1)	4841 (1)	3024 (1)	3156 (1)	73 (1)*
N(2)	4612 (3)	3428 (1)	3645 (2)	81 (1)*
N(3)	2114 (1)	3835 (1)	2892 (1)	85 (1)*
C(6)	5447 (3)	1568 (2)	1211 (3)	109 (1)
C(11)	5220 (2)	3541 (1)	4202 (2)	75 (1)
C(12)	5009 (3)	4026 (2)	4674 (2)	109 (1)
C(13)	5574 (3)	4182 (2)	5245 (2)	119 (1)
C(14)	6385 (2)	3848 (2)	5279 (2)	113 (1)
C(15)	6601 (4)	3392 (2)	4826 (3)	114 (1)
C(16)	6024 (2)	3231 (1)	4275 (1)	79 (1)
C(21)	2386 (2)	3202 (2)	3226 (2)	95 (1)
C(22)	1682 (3)	2849 (2)	3628 (3)	130 (1)
C(23)	2082 (4)	2245 (3)	3992 (3)	149 (2)
C(24)	1399 (4)	1931 (4)	4435 (4)	168 (2)
C(25)	1707 (3)	4295 (3)	3400 (3)	117 (1)
C(26)	2284 (5)	4536 (4)	4055 (4)	169 (2)
C(27)	1944 (6)	4918 (4)	4606 (4)	181 (2)
C(28)	1344 (6)	4685 (5)	5043 (4)	195 (3)
C(29)	2944 (4)	4101 (2)	2579 (3)	98 (1)
C(30)	2842 (4)	4767 (3)	2178 (4)	143 (1)
C(31)	3869 (5)	4873 (4)	2096 (4)	199 (3)
C(32)	3632 (8)	5266 (4)	1502 (6)	231 (4)
C(33)	1389 (2)	3715 (2)	2364 (2)	105 (1)
C(34)	1625 (4)	3283 (3)	1729 (3)	144 (2)
C(35)	774 (5)	3304 (3)	1345 (3)	151 (2)
C(36)	879 (6)	3006 (5)	814 (5)	218 (3)

[a] An asterisk denotes the equivalent isotropic U defined as one-third of the trace of the orthogonalized U_{eq} tensor.

Mo(8), and O(8). There are three structurally unique molybdenum centers: tetrahedral oxomolybdate units bridging through two oxo groups and occupying positions in the Mo_6O_6 girdle, distorted octahedral bis(diazenido)molybdenum centers $[MoO_4N_2]$ alternating with the $[MoO_4]$ units of the girdle, and the pseudotetrahedral oxomolybdate centers occupying the poles and bridging through three oxo groups.

The $[Mo_8O_{20}(NNPh)_6]^{4-}$ structure is related to that of the parent ion α-$[Mo_8O_{26}]^{4-}$, illustrated conventionally in Figure 4 and as a polyhedron model in Figure 5, and for which atomic positional parameters are presented in Table VI with selected bond lengths and angles in Table VI. The α-$[Mo_8O_{26}]^{4-}$ structure[21,22] can be viewed as a ring of six edge-shared $[MoO_6]$ octahedra capped on opposite faces by tripodal $[MoO_4]$ tetrahedra. Three of the oxo groups associated with each of the latter $[MoO_4]$ units are thus triply bridging, while the oxo groups of the $[Mo_6O_6]$ ring are doubly bridging. The $[Mo_8O_{20}(NNPh)_6]^{4-}$ structure may be derived from the α-$[Mo_8O_{26}]^{4-}$ structure by replacement of two terminal oxo groups on each of three alternate molybdenum atoms in the Mo_6O_6 crown by two phenyldiazenido groups and rotation of the capping $[MoO_4]$ units so as to shorten the Mo–O bridging distance to the diazenido-coordinated molybdenum centers (Mo(2), Mo(4), Mo(6)) at the expense of the interaction between the oxo groups of the capping units and the $[MoO_4]$ units of the ring (Mo(1), Mo(2), Mo(3)). Thus, whereas the average bond length of 2.451 (9) Å for the girdle molybdenum–triply bridging oxo group distance in α-$(n\text{-}Bu_4N)_4[Mo_8O_{26}]$ implies a bond order of less than 0.1, the significantly shorter bis(diazenido)molybdenum–capping oxo group average distance of 2.128 (3) Å corresponds to a bond order of ca. 0.5, with no significant interactions

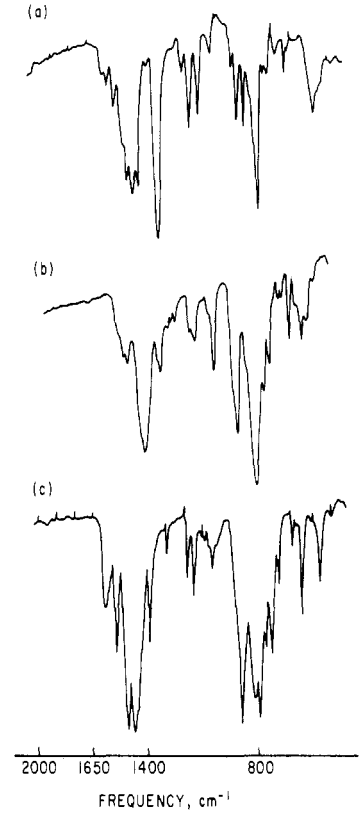

Figure 1. Infrared spectra in the 2000–500 cm^{-1} range: (a) $(n\text{-}Bu_4N)_2[Mo_4O_8(OMe)_2(NNC_6H_4\text{-}p\text{-}NO_2)_4]$; (b) $(n\text{-}Bu_4N)_2[Mo_4O_{10}(OMe)_2(NNPh)_2]$; (c) $(n\text{-}Bu_4N)_2(HNEt_3)_2[Mo_8O_{20}(NNPh)_6]$ (8% KBr pellets).

between these latter oxo groups of the capping $[MoO_4]$ center and the girdle $[MoO_4]$ units. An obvious effect of the diazenido coordination is the disruption of the edge-sharing of the girdle units of α-$[Mo_8O_{26}]^{4-}$ in favor of a less compact corner-sharing arrangement. Although this arrangement is unusual in view of arguments suggesting that edge-sharing by minimizing $M^{n+}\cdots M^{n+}$ repulsions stabilizes aggregation,[23,24] corner sharing of the bis-diazenido molybdenum octahedra $[MoO_4N_2]$ with bridging MoO_4 tetrahedral units is common to both octanuclear- and tetranuclear-derivatized complexes.

The three diazenido-derivatized molybdenum centers of the $[Mo_8O_{20}(NNPh)_6]^{4-}$ anion exhibit distorted octahedral geometry through coordination to the α-N donors of the diazenido groups, to two bridging oxo groups in the Mo_6O_6 girdle and to two bridging oxo groups from the capping $[MoO_4]$ units. Although the geometry is significantly distorted from the octahedral limit, these derivatized molybdenum centers display a considerably smaller displacement of the metal from the center of the vector connecting the pseudo-trans-bridging oxo groups of the $[Mo_6O_6]$ unit than that observed for α-$[Mo_8O_{26}]^{4-}$, as indicated by average O_b–Mo–O_b angles of 160.2 (1) and 143.1 (4)° for $[Mo_8O_{20}(NNPh)_6]^{4-}$ and $[Mo_8O_{26}]^{4-}$, respectively. The angular relaxation appears to reflect the less compact structure adopted by $[Mo_8O_{20}(NNPh)_6]^{4-}$ as a consequence of exclusive corner sharing of octahedra and tetrahedra. The short Mo–N and N–N distances of the bis(diazenido)molybdenum groupings are consistent with extensive delocalization throughout the Mo–N–N- unit, an observation also consistent with the linearity of the Mo–N–N moieties. Two distinct molybdenum–oxygen interactions for the $[MoO_4N_2]$ units emerge, reflected by Mo–O lengths of 2.020 (3) and 2.128 (3) Å for the distances to the oxygen donors in the girdle and to the capping oxygens, respectively. The longer bond distance may reflect a trans influence of the strongly π-bonding diazenido ligand.

(21) Day, V. W.; Frederick, M. F.; Klemperer, W. G.; Shum, W. *J. Am. Chem. Soc.* **1977**, *99*, 952.
(22) Fuchs, J.; Hartl, M. *Angew. Chem., Int. Ed. Engl.* **1976**, *15*, 375.
(23) Kepert, D. L. *Inorg. Chem.* **1969**, *8*, 1556.
(24) Gaiffon, A.; Spinner, B. *Rev. Chim. Miner.* **1975**, *12*, 316.

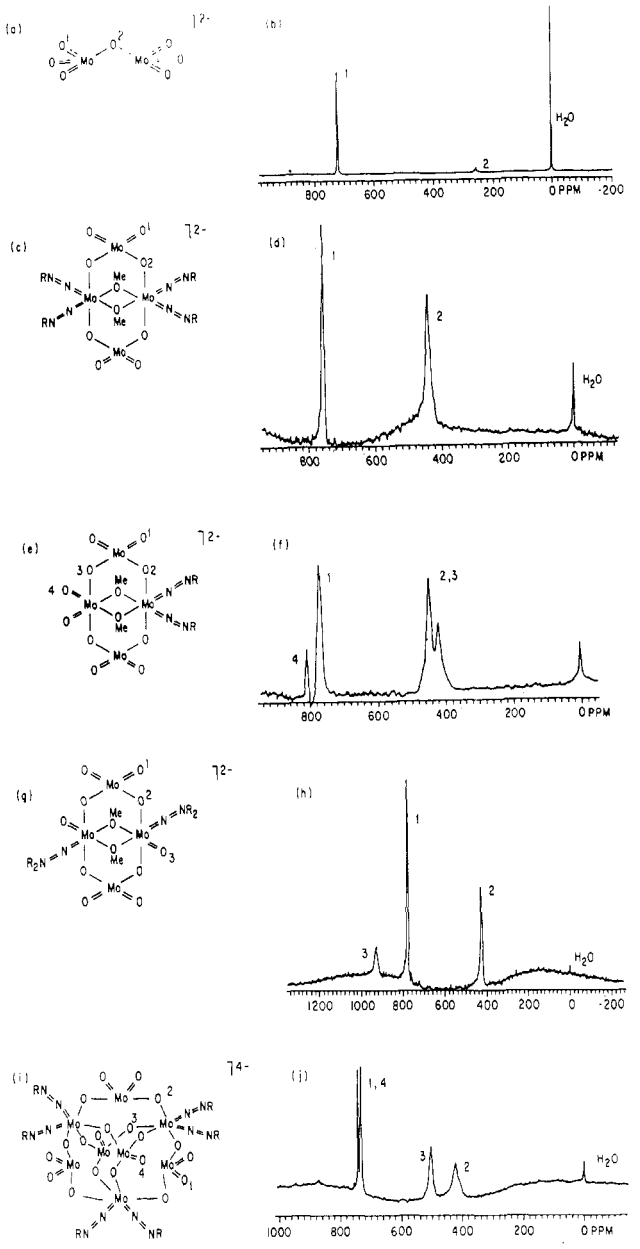

Figure 2. (a) Idealized bond structure of $[Mo_2O_7]^{2-}$, with one members from each set of equivalent oxygen atoms labeled. (b) ^{17}O NMR spectrum of $[Mo_2O_7]^{2-}$. (c) Idealized bond structure of $[Mo_4O_8(OMe)_2(NNAr)_4]^{2-}$, with one member from each set of equivalent oxygen atoms labeled. (d) ^{17}O NMR spectrum of $[Mo_4O_8(OMe)_2(NNAr)_4]^{2-}$. (e) Idealized bond structure of $[Mo_4O_{10}(OMe)_2(NNPh)_2]^{2-}$, with one member from each set of equivalent oxygen atoms labeled. (f) ^{17}O NMR spectrum of $[Mo_4O_{10}(OMe)_2(NNPh)_2]^{2-}$. (g) Idealized bond structure of $[Mo_4O_{10}(OMe)_2(NNPh_2)_2]^{2-}$, with one member from each set of equivalent oxygen atooms labeled. (h) ^{17}O NMR spectrum of $[Mo_4O_{10}(OMe)_2(NNPh_2)_2]^{2-}$. (i) Idealized bond structure of $[Mo_8O_{20}(NNPh)_6]^{4-}$, with one member from each set of equivalent oxygen atoms labeled. (j) ^{17}O NMR spectrum of $[Mo_8O_{20}(NNPh)_6]^{4-}$.

The geometry of the molybdenum centers of the octanuclear derivative $[Mo_8O_{20}(NNPh)_6]^{4-}$ may also be compared to those observed in the tetranuclear derivatives $[Mo_4O_8(OMe)_2(NNC_6H_4NO_2)_4]^{2-}$ and $[Mo_4O_{10}(OMe)_2(NNPh)_2]^{2-}$, shown in Figures 6 and 7. Tables VIII and X present the atomic positional parameters for $(n\text{-}Bu_4N)_2[Mo_4O_8(OMe)_2(NNC_6H_4\text{-}p\text{-}NO_2)_4]$ and $(n\text{-}Bu_4N)_2[Mo_4O_{10}(OMe)_2(NNPh)_2]$, respectively, while Tables IX and XI summarize selected bond lengths and angles. Since the $[Mo_4O_8(OR)_2(NNR)_4]^{2-}$ structural type has been discussed at length,[8] the structure is described herein only in relation to those of $[Mo_8O_{20}(NNPh)_6]^{4-}$ and $[Mo_4O_{10}(OMe)_2(NNPh)_2]^{2-}$. The structure of $[Mo_4O_8(OMe)_2(NNC_6H_4NO_2)_4]^{2-}$ consists of discrete

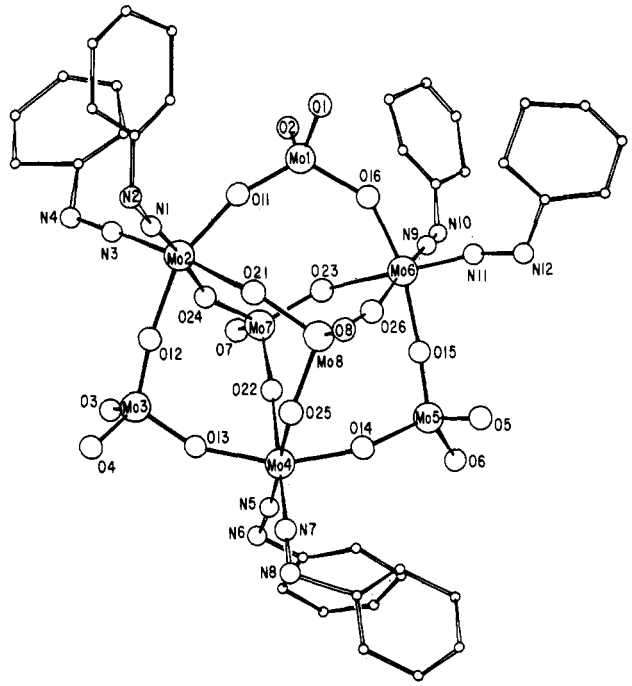

Figure 3. Perspective view of the $[Mo_8O_{20}(NNPh)_6]^{4-}$ structure giving the atom-labeling scheme used in the tables.

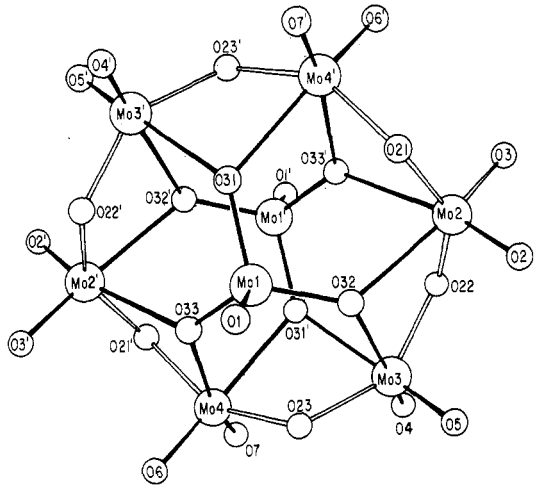

Figure 4. Perspective view of the structure of α-$[Mo_8O_{26}]^{4-}$ showing the atom-labeling scheme.

tetranuclear units, with a center of symmetry on the midpoint of the Mo(1)–Mo(3) vector imposing planarity on the Mo(1)–Mo(1′)–O(21)–O(21′) rhombus. The overall geometry may be viewed as two edge-sharing $[MoO_2(\mu\text{-}OMe)_2(NNAr)_2]$ octahedra, bridged by corner-sharing dipodal $[MoO_4]$ tetrahedra. The Mo_4O_4 heterocycle forms a puckered ring, elongated along the Mo(2)–Mo(2′) axis. The relevant bonding parameters for the derivatized molybdenum center $[MoO_4N_2]$ are summarized in Table XII and compared to those for the octanuclear derivative. The gross geometrical features of the $[MoO_4N_2]$ units are nearly identical, reflecting the structural requirements of the robust *cis*-bis(diazendo) core.

Structural parameters for the tetranuclear species $[Mo_4O_{10}(OMe)_2(NNPh)_2]^{2-}$ are summarized in Table XI. As illustrated in Figure 7, the overall structure consists of a $[MoO_4N_2]$ octahedral unit sharing an edge with the $[MoO_6]$ octahedron and bridged by dipodal $[MoO_4]$ tetrahedra. The crystallographic 2-fold axis coincident with the Mo(2)–Mo(3) vector imposes planarity on the Mo(2)–Mo(3)–O(6)–O(6′) rhombus and generates the symmetry-related halves of the tetranuclear unit. There are three chemically and crystallographically distinct molybdenum sites: the tetrahedral $[MoO_4]$ sites bridging the octahedral centers,

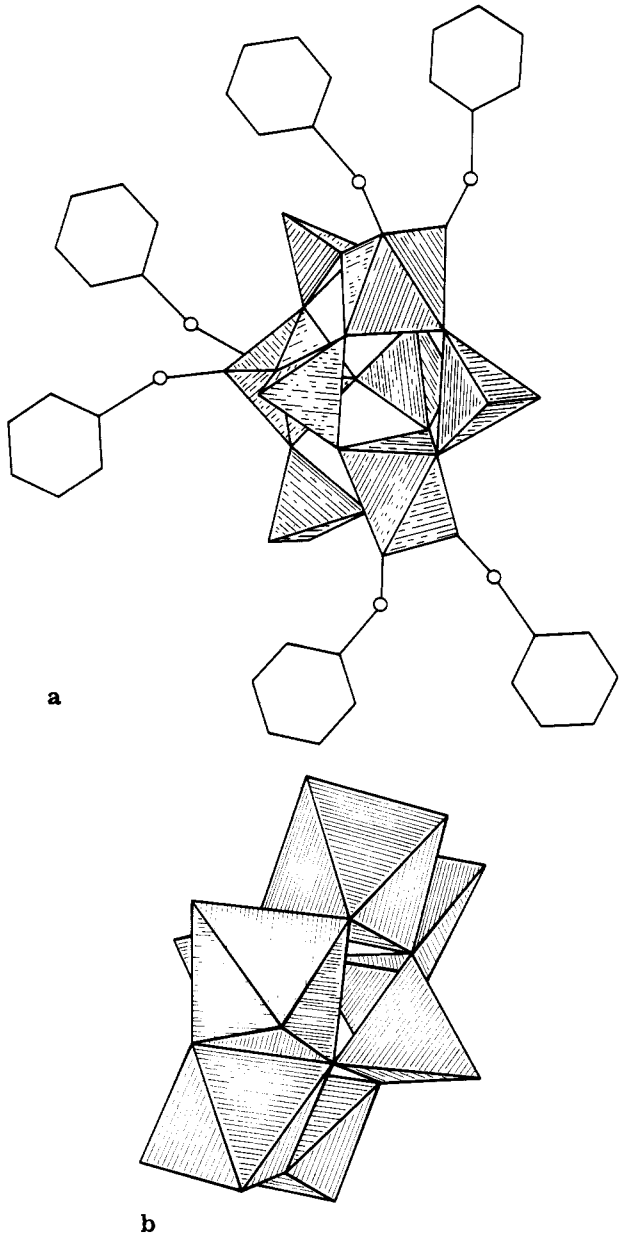

Figure 5. Idealized polyhedral models of (a) α-$[Mo_8O_{26}]^{4-}$ and (b) $[Mo_8O_{20}(NNPh)_6]^{4-}$.

Table XI. Bond Lengths (Å) and Angles (deg) for $(n\text{-}Bu_4N)_2[Mo_4O_{10}(OMe)_2(NNPh)_2]$

Mo(1)–O(1)	1.805 (3)	Mo(2)–O(6)	2.219 (3)
Mo(1)–O(2)	1.849 (2)	Mo(3)–O(1)	2.055 (2)
Mo(1)–O(3)	1.672 (3)	Mo(3)–O(6)	2.146 (3)
Mo(1)–O(4)	1.712 (3)	Mo(3)–N(1)	1.776 (2)
Mo(2)–O(2)	1.964 (2)	N(1)–N(2)	1.304 (7)
Mo(2)–O(5)	1.661 (3)	N(2)–C(11)	1.423 (7)
O(1)–Mo(1)–O(2)	111.6 (1)	O(2a)–Mo(2)–O(6a)	79.4 (2)
O(1)–Mo(1)–O(3)	106.9 (2)	O(5a)–Mo(2)–O(6a)	161.1 (2)
O(1)–Mo(1)–O(4)	111.5 (2)	O(1)–Mo(3)–O(6)	81.1 (2)
O(2)–Mo(1)–O(5)	94.7 (2)	O(1)–Mo(3)–N(1)	94.4 (2)
O(2)–Mo(1)–O(6)	79.4 (2)	O(1)–Mo(3)–O(1a)	165.7 (2)
O(2)–Mo(2)–O(2a)	160.5 (2)	O(1)–Mo(3)–O(6a)	87.1 (2)
O(2)–Mo(2)–O(5a)	97.3 (2)	O(1)–Mo(3)–N(1a)	95.8 (2)
O(2)–Mo(2)–O(6a)	84.3 (2)	O(6)–Mo(3)–N(1)	168.0 (2)
O(5)–Mo(2)–O(6)	161.1 (2)	O(6)–Mo(3)–O(1a)	87.1 (2)
O(5)–Mo(2)–O(2a)	97.3 (3)	O(6)–Mo(3)–O(6a)	69.7 (2)
O(5)–Mo(2)–O(5a)	103.9 (2)	O(6a)–Mo(3)–N(1a)	99.2 (2)
O(5)–Mo(2)–O(6a)	94.7 (2)	Mo(3)–N(1)–N(2)	171.7 (3)
O(6)–Mo(2)–O(2a)	84.3 (2)	Mo(1)–O(1)–Mo(3)	122.0 (3)
O(6)–Mo(2)–O(5a)	94.7 (2)	Mo(1)–O(2)–Mo(2)	127.0 (2)
O(6)–Mo(2)–O(6a)	67.1 (2)	Mo(2)–O(6)–Mo(3)	111.6 (2)
O(2a)–Mo(2)–O(5a)	94.7 (2)	N(1)–N(2)–C(11)	116.9 (3)

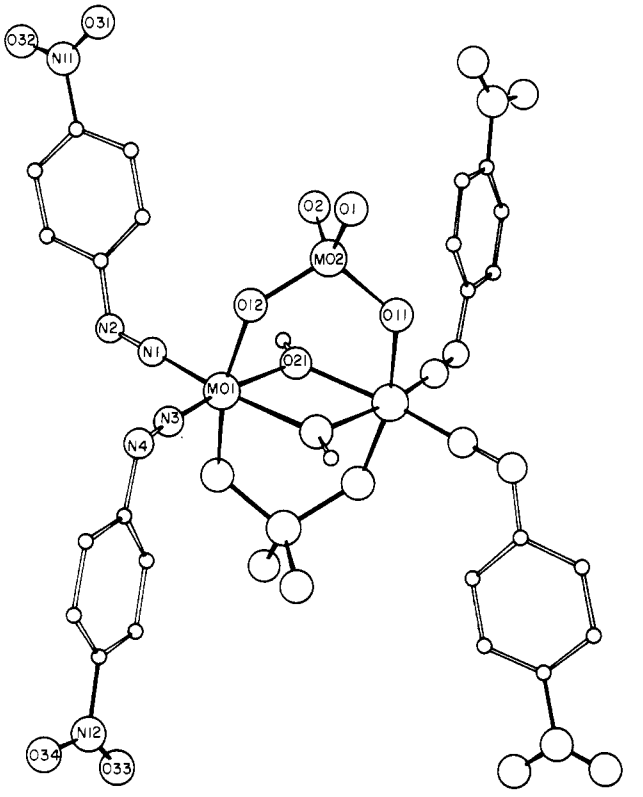

Figure 6. Perspective view of the structure of $[Mo_4O_8(OMe)_2(NNC_6H_4\text{-}p\text{-}NO_2)_4]^{2-}$, showing the atom-labeling scheme.

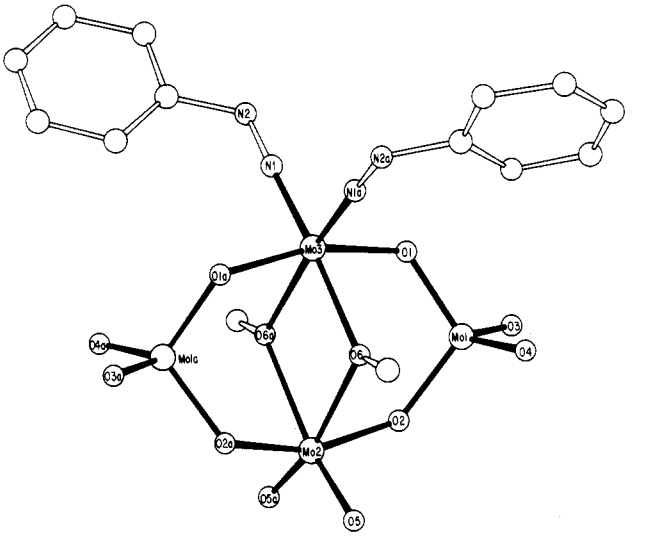

Figure 7. Perspective view of the structure of $[Mo_4O_{10}(OMe)_2(NNPh)_2]^{2-}$ giving the atom-labeling scheme used in the tables.

the diazenido-derivatized octahedral center, and the six-coordinate $[MoO_6]$ moiety.

The derivatized Mo site enjoys coordination to the α-nitrogen donors of the phenyldiazenido groups, to the bridging methoxy groups, and to the bridging oxygen donors of the $[MoO_4]$ units. The most unusual feature of the structure is the presence of the underivatized $[MoO_6]$ unit, with a molybdenum coordination consisting of two terminal oxo groups, two bridging methoxy donors, and two bridging oxo groups from the $[MoO_4]$ tetrahedral units.

The unsymmetrical pattern of methoxy group bridging, as shown by the Mo(2)–O(6) and Mo(3)–O(6) distances of 2.219 (3) and 2.146 (3) Å, respectively, is indicative of the significantly greater trans influence of the oxo group than of the phenyldiazenido moiety. The geometry of the *cis*-bis(diazenido)molybdenum center of $[Mo_4O_{10}(OMe)_2(NNPh)_2]^{2-}$ is essentially

Table XII. Comparison of Selected Bonding Parameters for Octanuclear and Tetranuclear Molybdenum Complexes of This Study[a]

	$(n\text{-}Bu_4N)_4[Mo_8O_{26}]$	$(NHEt_3)_2(n\text{-}Bu_4N)_2[Mo_8O_{20}(NNPh)_6]$	$(n\text{-}Bu_4N)_2[Mo_4O_8(OMe)_2(NNC_6H_4\text{-}p\text{-}NO_2)_4]$	$(n\text{-}Bu_4N)_2[Mo_4O_{10}(OMe)_2(NNPh)_2]$
$Mo\text{–}O_t$[b]	1.695 (9)	1.732 (5),[c] 1.677 (6)[d]	1.706 (9)	1.672 (4),[c] 1.661 (3)[e]
$Mo_c\text{–}O_{3b}$	1.778 (9)			
$Mo_c\text{–}O_{2b}$		1.752 (7)	1.808 (5)	1.827 (5)
$Mo\text{–}O_{2b}$	1.905 (9)	1.796 (8),[f] 2.020 (8),[g] 2.128 (7)[h]	2.047 (6)	1.964 (2),[i] 2.055 (2)[j]
Mo–O(methoxy)			2.141 (6)	2.219 (3),[i] 2.146 (3)[j]
$Mo\text{–}O_{3b}$	2.451 (9)			
Mo–N		1.802 (9)	1.816 (9)	1.776 (3)
$O_{2b}\text{–}Mo\text{–}O_{2b}$	143.1 (4)	160.2 (4)	165.7 (2)	160.5 (2),[i] 165.7 (3)[j]
N–Mo–N		90.1 (5)	94.4 (3)	92.2 (2)

[a] Bond lengths in Å, angles in deg. [b] Abbreviations: O_t, terminal oxo group; Mo_c, capping tetrahedral molybdenum center; O_{3b}, triply bridging oxo group; O_{2b}, doubly bridging oxo group. [c] $Mo\text{–}O_t$ for capping MoO_4 unit. [d] $Mo\text{–}O_t$ for MoO_4 unit of the Mo_6O_6 crown. [e] Octahedral MoO_6 site. [f] $Mo\text{–}O_{2b}$ for crown MoO_4 unit. [g] $Mo\text{–}O_{2b}$ for crown O_{2b} units to the MoO_4N_2 octahedral site. [h] $Mo\text{–}O_{2b}$ for capping O_{2b} units to the MoO_4N_2 octahedral sites. [i] Octahedral MoO_4 site. [j] Octahedral MoO_4N_2 site.

identical with the $[MoO_4N_2]$ coordination sites of $[Mo_4O_8(OMe)_2(NNPh)_4]^{2-}$ and $[Mo_8O_{20}(NNPh)_6]^{4-}$, as illustrated in Table XII.

Conclusions. The *cis*-bis(diazenido)molybdenum unit $[Mo(NNR)_2]^{2+}$ is a chemically robust core that persists in a variety of solvents and synthetic conditions and provides a nucleus for aggregation in cluster formation. The molybdenum center of the $[Mo(NNR)_2]^{2+}$ unit typically exhibits pseudooctahedral coordination geometry of the type $[MoO_4N_2]$ in these derivatized isopolymolybdate clusters.

Both the octanuclear species $[Mo_8O_{20}(NNPh)_6]^{4-}$ and the tetranuclear dinegative anions $[Mo_4O_8(OMe)_2(NNC_6H_4NO_2)_4]^{2-}$ and $[Mo_4O_{10}(OMe)_2(NNPh)_2]^{2-}$ are unusual in that $[MoO_4]$ tetrahedra provide the polymolybdate framework, rather than the $[MoO_6]$ octahedral units, which are exclusively found in other derivatized polymolybdates.[3-6] Whereas these latter structures are representatives of clusters based on edge-shared $[MoO_6]$ octahedra and conform to the empirical "rules of compactness", the diazenido derivatives are constructed from corner-sharing $[MoO_4]$ tetrahedra and $[MoO_4N_2]$ units, resulting in a less compact aggregate. The diazenido derivatives $[Mo_8O_{20}(NNPh)_6]^{4-}$, $[Mo_4O_8(OMe)_2(NNPh)_4]^{2-}$, and $[Mo_4O_{10}(OMe)_2(NNPh)_2]^{2-}$ may be accurately represented by the respective formulations $(MoO_4^{2-})_2[Mo_6O_{12}(NNPh)_6]^{2+}$, $(MoO_4^{2-})_2[Mo_2(OMe)_2(NNPh)_4]^{2+}$, and $(MoO_4^{2-})_2[Mo_2O_2(OMe)_2(NNPh)_2]^{2+}$, which characterize the weak interactions between the capping $[MoO_4]^{2-}$ ions and the central cores of these clusters.

The low bond orders of the interactions of the core units with the capping $[MoO_4]^{2-}$ tetrahedra suggest kinetic lability and may point toward mechanistic pathways for reactions involving these aggregates. The capping groups of the $[Mo_4O_8(OMe)_2(NNR)_4]^{2-}$ cluster types, for example, are readily displaced to give complexes of the type $[Mo_2(OMe)_2(NNR)_4L_2L'_2]$ where $L = -Cl^-$ or $-OR^-$ and $L' = H_2NNHPh$ or HOR.

Although the structural systematics of the diazenido-derivatized polymolybdates are beginning to emerge, the mechanisms of formation and aggregation of these species remain unclear. The structures suggest that formation involves simple addition of $[MoO_4]$ tetrahedra to a molybdenum–diazenido core of the $[MoO_2N_2]$ type. In contrast to isopolytungstate formation where a WO_4 unit acts as a bidentate ligand to a single WO_4 unit, thereby expanding the coordination number to six,[25] the $[MoO_4]$ units act as corner-sharing tetrahedra bridging two or more *cis*-bis(diazenido)molybdenum units to produce the less compact aggregates described in this report. This unusual pattern of aggregation may also reflect the incorporation of molybdenum centers in a formal oxidation state other than VI. The metal–diazenido moieties of these structures display metrical parameters consistent with the description of the phenyldiazo unit as the three-electron-donating $-N_\beta R^+$ structure.[26,27] Thus, the derivatized molybdenum centers may be considered, in a formal sense, to be Mo(0). Alternatively, the aryldiazenido(1–) formalism produces an oxidation state of IV for the derivatized molybdenum centers. In this respect, it is unusual that the clusters do not exhibit well-behaved electrochemical oxidation processes but rather present poorly resolved irreversible redox processes common to type II polymetalate structures.[28]

Acknowledgment. We are grateful to the National Science Foundation for financial support (Grant No. CHE8514634 to J.Z.).

Registry No. **1**, 110773-14-3; **2**, 59054-50-1; **3**, 110773-16-5; **4**, 110773-18-7; $(n\text{-}Bu_4N)_2[Mo_4O_{10}(OMe)_2(NNPh_2)_2]$, 105473-71-0; $(n\text{-}Bu_4N)[Mo_8O_{20}(NNPh)_6]$, 110773-19-8.

Supplementary Material Available: Tables S1, S5, S10, and S15, listing bond distances for **1–4**, Tables S2, S6, S11, and S16, listing bond angles for **1–4**, Tables S3, S7, S12, and S17, listing anisotropic thermal parameters for **1–4**, and Tables S8, S13, and S18, listing hydrogen atom parameters for **2–4** (26 pages); tables of calculated and observed structure factors for **1–4** (Tables S4, S9, S14, and S19) (222 pages). Ordering information is given on any current masthead page.

(25) Kepert, D. L. *Prog. Inorg. Chem.* **1962**, *4*, 199.
(26) Sutton, D. *Chem. Soc. Rev.* **1975**, *4*, 443.
(27) Hillhouse, G. L.; Haymore, B. L.; Bistram, S. A.; Hermann, W. A. *Inorg. Chem.* **1983**, *22*, 314.
(28) Pope, M. T. *Inorg. Chem.* **1972**, *8*, 1973.
(29) Chisholm, M. H.; Folting, K.; Huffman, J. C.; Kirkpatrick, C. C. *Inorg. Chem.* **1984**, *23*, 1021.